THE UNIVERSITY of EDINBURGH

Edinburgh Research Explorer

Neurotrophin p75 receptor (p75NTR) promotes endothelial cell apoptosis and inhibits angiogenesis

Link:
Link to publication record in Edinburgh Research Explorer

Document Version:
Peer reviewed version

Published In:
Circulation Research

OPEN ACCESS

The neurotrophin receptor p75NTR triggers endothelial cell apoptosis and inhibits angiogenesis: implications for diabetes-induced impairment of reparative neovascularization

Andrea Caporali[1,*], **Elisabetta Pani**[1,2,*], **Anton J. G. Horrevoets**[3], **Nicolle Kraenkel**[1], **Atsuhiko Oikawa**[1], **Graciela B. Sala-Newby**[4], **Marco Meloni**[1], **Brunella Cristofaro**[1], **Gallia Graiani**[5], **Aurelie Leroyer**[6], **Chantal Boulanger**[6], **Andrew Herman**[7], **Gaia Spinetti**[2], **Sung Ok Yoon**[8], **Paolo Madeddu**[1], and **Costanza Emanueli**[1]

[1]*Experimental Cardiovascular Medicine, University of Bristol, Bristol, United Kingdom* [2]*IRCCS Multimedica Hospital, Milan, Italy* [3]*Biochemistry, Academic Medical Center, University of Amsterdam, Netherlands* [4]*Vascular Biology, Bristol Heart Institute, University of Bristol, Bristol, United Kingdom* [5]*Pathology, University of Parma, Italy* [6]*INSERM Cardiovascular Research Center, Hôpital Lariboisière, Paris, France* [7]*Molecular and Cellular Medicine, University of Bristol, Bristol, United Kingdom* [8]*Center for Molecular Neurobiology, Ohio State University, OH, USA*

Abstract

Diabetes compromises endothelial function and inhibits reparative neovascularization. The neurotrophin receptor p75NTR is scarcely present in healthy endothelial cells (EC), but diabetes induces p75NTR in capillary EC of ischemic limb muscles. Here, we show that forced *p75NTR* expression impairs survival, proliferation, migration, and adhesion capacities of EC and endothelial progenitor cells (EPC) and inhibits EC tube formation. In EC, *p75NTR* depresses the VEGF-A/Akt/ eNOS/NO pathway and reduces *VEGF-A, ITGB1*, *BIRC5*, *PTTG*1, and *VEZF1* mRNA levels. Moreover, both diabetes and *p75NTR* transfer down-regulate *VEGF-A, ITGB1,* and *VEZF1* in adductor muscles. Forced *p75NTR* expression by ischemic limb muscles impairs post-ischemic neovascularization and blood flow recovery in normoglycemic mice. Conversely, p75NTR inhibition in diabetic muscles restores proper post-ischemic neovascularization and prevents apoptosis of muscular capillary EC and bone marrow-resident Sca-1$^+$Lin$^-$ progenitor cells. Collectively, our data identify the anti-angiogenic action of p75NTR and suggests the therapeutic potential of p75NTR inhibition to combat diabetes-induced microvascular liabilities.

Diabetes induces apoptosis and reduces the function of endothelial cells (EC) and endothelial progenitor cells (EPC). As a result, post-ischemic reparative angiogenesis and vasculogenesis are both impaired in diabetic subjects.[1-12] The consequences are harmful: In the leg, severe microangiopathy aggravates atherosclerosis-induced muscular ischemia, thus contributing to gangrene and cutaneous ulcers with a severely impaired healing potential, which make amputation of the diabetic foot an all-too-frequent necessity.[13,14] A remedy to prevent and treat such diabetic microvascular complications is urgently needed.

Corresponding Author: Costanza Emanueli, BSc, PhD, FAHA, Bristol Heart Institute, University of Bristol, Bristol Royal Infirmary, level 7, Upper Maudlin Road, BS2 8HW Bristol, UK, Phone: ++ 44 (0)117 9283512, Fax: ++ 44 (0)117 9283904, Emails: Costanza.Emanueli@bristol.ac.uk or c.emanueli@yahoo.co.uk.
*Authors contributed equally.

Neurotrophins (NTs) have been extensively studied for their actions on the nervous system. However, it is becoming increasingly evident that the expression and function of NTs is also important in the cardiovascular system. Both EC and EPC express tropomyosin kinase receptors (trk), which are tyrosine-kinases binding NTs with high affinity. The NT nerve growth factor (NGF) and brain-derived neurotrophic factor (BDNF), acting on trkA and trkB respectively, promote EC survival and angiogenesis.[3,15-18] Moreover, NGF, *via* trkA, is an autocrine survival factor for cardiomyocytes.[19] NTs have another receptor of 75 KD MW (p75[NTR]). p75[NTR] contains a death domain and belongs to the TNF receptor super-family, but it does not bind TNF-α. In neural cells, p75[NTR] mediates apoptosis and cell cycle arrest.[20-22] It was proposed that p75[NTR] has a low affinity for mature NTs, as it preferentially binds pro-forms of NTs.[23-25] However, the mechanisms underpinning p75[NTR] activation and downstream molecular signaling have not been fully elucidated. Notably, no investigation of the role of p75[NTR] on EC and EPC survival and function or on blood vessel growth has been attempted to date. We previously reported that p75[NTR] is scarce in capillary EC of healthy murine limb muscles, but that expression strikingly increases following induction of type-1 diabetes and hindlimb ischemia; two conditions that also promote EC apoptosis.[3,10,26]

This study demonstrates that p75[NTR] promotes apoptosis of EC and vascular progenitor cells and inhibits neovascularization. We explain the anti-angiogenic effect of p75[NTR] by its inhibitory effect on the vascular endothelial growth factor A (VEGF-A)/Akt kinase axis. Finally, we provide evidence that p75[NTR] is responsible for the impaired neovascularization response to peripheral ischemia in diabetes.

Results

Adenovirus-mediated p75[NTR] transduction of EC

Under standard culture conditions, human umbilical vein EC (HUVEC) have insignificant p75[NTR] expression level (see *Null* group of Fig. 1a and 1b,). To study p75[NTR] functions in EC we forced the expression of the human *p75[NTR]* or *Null* control in HUVEC by adenovirus-mediated gene transfer. Successful *p75[NTR]* transduction was confirmed by both western blot and FACS analysis (Fig. 1a and 1b).

p75[NTR] promotes EC apoptosis

Next, we studied the impact of increased p75[NTR] expression on HUVEC survival. FACS analysis showed that p75[NTR] expression precedes appearance of apoptosis in *p75[NTR]*–transduced HUVEC (*p75[NTR]*–HUVEC) (Fig. 1b and 1c). Early apoptosis (cells positive for Annexin-V and negative for propidium iodide (PI)) peaked at 24h, followed, at 48h, by late apoptosis (Annexin-V[+]PI^{+} cells). We confirmed the pro-apoptotic effect of p75[NTR] in HUVEC by TUNEL apoptosis assay (Fig. 1d), western blot for the apoptosis marker cleaved (activated) caspase-3 (Fig. 1a), and caspase-3 activity assay (Fig. 1e). Additionally, we measured the release of endothelial apoptotic microparticles (EMP)[27-29] from *p75[NTR]* and *Null*-transduced HUVEC (*Null*-HUVEC) with or without exposure to the apoptosis inducer staurosporin (100nM, 16h). Under both circumstances, p75[NTR] enhanced EMP release and p75[NTR] was present in EMP (Fig. 1g). Taken together, these results demonstrate that p75[NTR] promotes HUVEC apoptosis, *via* caspase-3 activation, in a concentration-response manner. The pro-apoptotic effect of p75[NTR] was confirmed on human microvascular EC (MVEC) (Fig. 1f).

There is no consensus as to whether p75[NTR] needs ligand activation to start its death signal. We investigated this possibility on *p75[NTR]*- or *Null*-HUVEC by adding recombinant proNGF, NGF, or BDNF. Both proNGF and NGF slightly increased apoptosis in *p75[NTR]*-HUVEC but not *Null*-HUVEC (Fig. 1h). By contrast, in this experimental setting, BDNF did not influence apoptosis. To rule out the possibility that endogenously produced ligands cause apoptosis

via p75[NTR], we cultured *p75[NTR]*-HUVEC and *Null*-HUVEC in the presence of a NGF neutralizing antibody[3,19] or a soluble trkB receptor.[17] Blockade of endogenous NGF or BDNF did not alter apoptosis rate (data not shown). This series of results suggests that p75[NTR] can induce EC apoptosis *via* both ligand-dependent and -independent mechanisms.

p75[NTR] impairs EC proliferation, migration, and *in vitro* angiogenesis

In neural cells, p75[NTR] promotes cell cycle arrest.[20] Since EC replication is intrinsic to the angiogenesis process, we studied the impact of p75[NTR] on HUVEC cycle progression. HUVEC were synchronized at G_1/S boundary by serum starvation and the progression of cell cycle upon release from the G_1-block was analyzed by flow cytometry. As shown in Fig. 2a, the control *Null*-HUVEC entered the cell cycle and progressed through S-phase and G2-M. *p75[NTR]*-HUVEC were delayed in cycling, as shown by the reduced percentage of cells in S-phase (P<0.01 at 21h). Correspondingly, the level of phosphorylated tumor suppressor retinoblastoma protein (Rb), a marker of cell cycle progression,[30] was less in *p75[NTR]*-HUVEC (Fig. 2b). The anti-proliferative effect of p75[NTR] on EC was further confirmed by BrdU incorporation assay (Fig. 2c).

EC migration is essential for neovessel formation. We tested the effect of *p75[NTR]* on EC migratory capacity toward stroma derived factor-1 (SDF-1), which is a classic chemotactic stimulus for the cells of the endothelial lineage.[31,32] At both 12h and 48h from transduction, SDF-1 promoted migration of *Null*-HUVEC. By contrast, the migratory capacity of *p75[NTR]*-HUVEC to SDF-1 was severely impaired (Fig. 2d for 48h; 12h data not shown).

Cell-matrix adhesion is also fundamental for vessel growth and maintenance. At both 12h and 48h from transduction, *p75[NTR]*-HUVEC showed reduced adhesion capacity to fibronectin (Fig. 2e for 48h; 12h data not shown).

Finally, we tested the angiogenic potential of *p75[NTR]*-HUVEC by performing a matrigel assay, which allows determination of the EC potential to give rise to blood vessel-like tubular structures *in vitro*, thus mimicking angiogenesis. In this assay, which was initiated at 12h post-gene transfer and carried out in the presence of growth factors, the anti-angiogenic effect of p75[NTR] was evident (Fig. 2f).

p75[NTR] impairs EPC survival and functions

The growth of new blood vessels needs the participation of both angiogenesis, developed by pre-existing vessels, and vasculogenesis, which involves EPC. Therefore, we extended our study to human peripheral blood EPC. As shown in supplementary Fig. 1, p75[NTR] negatively impacted on EPC survival (activated caspase-3 assay, panel b), proliferation (FACS analysis of BrdU incorporation, panel c), migration toward SDF-1 (panel d), and adhesion (data not shown).

p75[NTR] induces a pro-apoptosis and anti-angiogenesis signalling pathway in EC

p75[NTR] transduction decreased VEGF-A and Ser473-phospho-Akt levels in HUVEC (Fig. 3a). Phospho-Akt positively controls EC survival and angiogenesis by several downstream mediators, including endothelial nitric oxide synthase (eNOS).[33] Correspondingly, we found that *p75[NTR]* transduction impaired Ser1177-phosphorylation of eNOS (Fig. 3a) and eNOS-derived NO production (Fig. 3b). Normal phospho-eNOS content was restored by gene delivery of either *VEGF-A* or a constitutive active Akt mutant form (*Myr-Akt*) in *p75[NTR]*-HUVEC (Fig. 3c). By contrast, *Myr-Akt* did not rescue VEGF-A level in *p75[NTR]*-HUVEC, thus suggesting that VEGF-A lies upstream of Akt phosphorylation (Fig. 3c). Focal adhesion kinase (FAK), upstream of Akt, controls EC migration, proliferation and survival.[34] Phospho (active)-FAK was less in *p75[NTR]*-HUVEC and, as expected, *Myr-Akt* did not restore phospho-FAK to normal

levels (Fig 3c). By contrast, *VEGF-A* increased phospho-FAK in *p75^NTR*-HUVEC (Fig. 3c). In EPC, p75^NTR reduced the levels of both phospho-Akt and phospho-eNOS (supplementary Fig. 1d).

To investigate the role of depressed VEGF-A and phospho-Akt in the anti-angiogenic action of p75^NTR, we performed a rescue experiment in the matrigel assay model. The capacity of *p75^NTR*-HUVEC to form tubular structures was restored by either *VEGF-A* or *Myr-Akt* (Fig. 3d), suggesting that the anti-angiogenic action of *p75^NTR* is caused by inhibition of the VEGF-A/Akt pathway.

p75^NTR downregulates *BIRC5* and *PTTG1* mRNA levels in EC

To further understand the p75^NTR-induced molecular program contributing to EC apoptosis and anti-angiogenesis, we performed a GeArray for apoptosis and cell cycle-related genes on mRNA extracted from *p75^NTR*-HUVEC and *Null*-HUVEC. Results (not shown) were confirmed by real time RT-PCR. As shown in Fig. 3e, *p75^NTR* reduced the mRNA expression of *BIRC5* (survivin) and pituitary tumor-derived transforming gene (*PTTG1*, also named securin), which are pro-angiogenic and pro-EC survival mediators transcriptionally controlled by phospho-Akt.[35,36] Accordingly, *Myr-Akt* increased *BIRC5* and *PTTG1* in *p75^NTR*-HUVEC.

Expressional changes induced by p75^NTR over-expression in limb muscles confirm the activation of an anti-angiogenesis program, which is also present in diabetic muscles

We previously found that p75^NTR expression by capillary EC correlated with apoptosis and with reduced capillary density.[3,37] Here, we have employed full genome expression profiling using Illumina bead-arrays interrogating 46,600 murine genome transcripts to study the global impact of *p75^NTR* transduction on the gene expression program of normoperfused murine muscle. The overall changes in the transcriptome were analyzed at the levels of specific functional pathways using Panther-annotated protein group analysis.[38] This analysis identified, in addition to a number of inflammatory or muscle-specific pathways (data not shown), a specific, statistically significant reduction in gene-sets involved in endothelial survival and angiogenesis processes, i.e. VEGF-signalling and integrin-signalling. Analysis of the corresponding genes in more detail identified 3 pivotal genes (*VEGF-A*, *ITGBL1*, *VEZF1*) that were suppressed by *p75^NTR*, relative to a number of well-established endothelial-specific genes (data not shown). By real-time RT-PCR, we confirmed that *p75^NTR* alters the expression of *VEGF-A*, *ITGBL1* and *VEZF1* in both murine muscles and HUVEC (Figs. 3f and 3g). Notably, muscular expression of *VEGF-A*, *ITGBL1* and *VEZF1* is dramatically down-regulated by diabetes (Fig. 3f). *VEGF-A* transfer corrected *ITGB*, but not *VEZF1* deficit in *p75^NTR*-HUVEC. The scheme in Fig 3h illustrates our interpretation of the molecular change induced by p75^NTR in EC.

p75^NTR impairs post-ischemic neovascularization and blood flow (BF) recovery in a mouse model of limb ischemia

To test the impact of *p75^NTR* on blood vessel growth in ischemic limb muscles, *Ad.p75^NTR* (V5-tagged) or *Ad.Null* was injected into the ischemic adductor of normoglycemic mice. We verified successful gene transfer by western blot analysis for p75^NTR (Fig. 4a). By immunohistochemistry for V5 (red fluorescence), we observed localization of the transgene in capillary EC (recognized by FITC-isolectin staining –green fluorescence-) of the ischemic muscles (Fig. 4b). Limb BF was measured by colour laser Doppler at 0, 7, and 14d post-ischemia. A severe delay in BF recovery was observed in the *p75^NTR* group (Fig. 4c for 14d post-ischemia; other data not shown). Correspondingly, capillary density was reduced in *p75^NTR*-over-expressing muscles (Fig. 4d). In additional mice sacrificed at 5d post-ischemia, which, in comparison to 14d, is a time-point more informative on ischemia-induced EC

proliferation and apoptosis, we observed that p75[NTR] induces apoptosis (Fig. 4e) and inhibits proliferation (Fig. 4f) of capillary EC. Interestingly, intramuscular *Ad.p75[NTR]* increased the abundance of apoptotic Sca-1+Lin- cells resident in the ipsilateral limb BM (Fig. 4g and 4e). Sca-1+Lin- represents a murine progenitor cell population able to give rise to EC.[39,40] To determine whether Sca-1+Lin- cell apoptosis was associated with transgene expression in the BM, we searched for V5 in BM (by western blot), but we did not find it. To further investigate whether gene delivery to ischemic muscles can infect BM-resident cells, we injected muscles with *Ad.GFP* and, after 3d, we performed FACS analysis for GFP fluorescence of total BM cells. We did not detect any GFP fluorescence (data not shown). These experiments disclaim the possibility of *p75[NTR]* transduction of BM cells following intramuscular gene delivery.

Diabetes increases p75[NTR] expression and apoptosis of BM-resident progenitor cells

Extending our previous findings of an association between diabetes, p75[NTR] expression and apoptosis in EC,[3] we provide new evidence that – even in the absence of superimposed ischemia - diabetes increases the abundance of both Sca-1+p75[NTR+] (Fig. 5a) and Sca-1+Lin- p75[NTR+] cells (Fig. 5c) in limb BM. Diabetic Sca-1+p75[NTR+] cells expressed the apoptosis marker Annexin-V (Fig. 5 d, e, f). These data suggest a role for p75[NTR] in diabetes-induced progenitor cell apoptosis.

Blocking p75[NTR] re-establishes proper post-ischemic neovascularization and BF recovery in diabetic mice undergoing peripheral ischemia

We finally tested the hypothesis that p75[NTR] plays a major role in diabetes-induced impaired neovascularization response to limb ischemia. This was accomplished in diabetic mice by investigating whether blocking p75[NTR], using an adenovirus carrying a dominant negative mutant form of *p75[NTR]* (*Ad.DN-p75[NTR]*), restores proper post-ischemic neovascularisation and BF recovery. Supplementary Fig. 2 confirms our previous data of increased p75[NTR] expression by capillary EC in ischemic muscles of diabetics in comparisons to normoglycemic mice.[3] As shown in Fig. 6a, foot BF recovery overtime was impaired in diabetic mice receiving the control virus *Ad.GFP*. *Ad.DN-p75[NTR]* had no effect in normoglycemic mice, whereas it improved BF recovery in diabetic mice, making it comparable to that of normoglycemic controls. Representative Doppler images of hindlimbs at 15d post-ischemia are presented (Fig. 6b). We observed a similar trend when measuring intra-muscular BF (Fig. 6c). Additionally, post-ischemic clinical outcome (calculated as the number of auto-amputated or necrotic fingers in the ischemic foot)[9,41] was worsened by diabetes. Notably, *Ad.DN-p75[NTR]* improved the clinical outcome of diabetic mice (number of necrotic/amputated fingers at 15d: 1.6 ± 0.9 in diabetic with *Ad.DN-p75[NTR]*.vs. 3.7 ± 0.9 in diabetic with *Ad.GFP,* P<0.05 and vs. 1.4 ± 0.7 in healthy with *Ad.GFP*, P=N.S.). As shown in Fig. 6d, the capillarization response to ischemia was not altered by *Ad.DN-p75[NTR]* in normoglycemic mice. Diabetes impaired post-ischemic neovascularization, with this effect being prevented by *Ad.DN-p75[NTR]*. Furthermore, *Ad.DN-p75[NTR]* improved EC proliferation (assessed by MCM-2 staining[42] -Fig 6e-) and inhibited EC apoptosis (TUNEL assay -Fig. 6f-) in diabetic muscles. Notably, intra-muscular *Ad.DN-p75[NTR]* reduced Sca-1+Lin- cell apoptosis in the diabetic BM (Fig. 6g and 6h).

Discussion

We previously showed and confirm here that diabetes induces p75[NTR] expression in capillary EC belonging to ischemic limb muscles[3]. With this study, we provide evidence that p75[NTR] induces apoptosis of EC and EPC and severely impairs their pro-angiogenesis function. The apoptotic and cell cycle inhibitor effects of p75[NTR] on neural cells were already known.[20-22] In neural cells, p75[NTR] plays an ambiguous "Jekyll-and-Hyde" role, being able to either kill or stimulate cell survival and differentiation.[21,22] By contrast, according to our findings, p75[NTR] has only detrimental actions on cells belonging to the endothelial lineage.

We have showed the strong anti-neovascularization effect of p75[NTR] in a mouse model of limb ischemia. In normoglycemic mice, *p75[NTR]* transduction of ischemic muscles enhanced apoptosis and reduced proliferation of capillary EC, thus ultimately depressing post-ischemic neovascularization and BF recovery. Interestingly, *p75[NTR]* transduction of muscles enhanced apoptosis of BM-resident Sca-1^{+}Lin^{-} progenitor cells. Since we were able to exclude the possibility that the transgene penetrated the BM, we are encouraged to speculate that the increase in apoptosis of BM-resident progenitor cell may be due to more severe limb ischemia following *p75[NTR]* over-expression.

Conclusive proof that p75[NTR] is responsible for diabetes-induced impaired reparative neovascularization is provided by the experiment in which p75[NTR] activity in ischemic limb muscles was blocked by a dominant negative *p75[NTR]* mutant form. Whilst the *p75[NTR]* dominant negative had no effects in normoglycemic mice, it inhibited EC apoptosis, normalized EC proliferation, and restored proper muscular capillarization and BF recovery in diabetic mice. Notably, blocking *p75[NTR]* in diabetic limb muscles additionally resulted in survival of BM-resident Sca-1^{+}Lin^{-} progenitor cells. This is in line with the observed increased apoptosis of BM cells following muscular *p75[NTR]* over-expression.

Overall, our *in vivo* findings have important clinical implications and may help to design innovative therapeutic approaches able to promote angiogenesis and vasculogenesis in a diabetic context.

Notably, the molecular signalling pathways that we identified to be downstream of p75[NTR] in EC totally differ from those previously described in neural cells. In fact, we newly report here that p75[NTR] inhibits the VEGF-A/Akt/eNOS/NO pathway. This is probably the most relevant pathway for angiogenesis and EC survival[33,43] and its deficit may *per se* justify the impairment of EC function. In line with this hypothesis, co-transduction with either *VEGF-A* or *Myr-Akt* rescued the capacity of *p75[NTR]*-HUVEC to form vascular-like tubular structures on matrigel. Moreover, *Myr-Akt* improved survival of *p75[NTR]*-HUVEC (unpublished data, 2007). Phospho-Akt positively regulates the transcription of *BIRC5*[35] and *PTTG1*,[36] which resulted in both being downregulated by *p75[NTR]*. Notably, *Myr-Akt* totally or partially rescued *BIRC5* and *PTTG1* mRNA expression levels in *p75[NTR]*-HUVEC. BIRC5, which was named survivin for its pro-survival action, was recently discovered to be a positive mediator of angiogenesis.[35,44,45] Interestingly, BIRC5 also modulates cell cycle entry by interaction with Cdk4 and activation of Cdk2/Cyclin E complex leading to Rb phosphorylation.[46] This may be reconciled with the impaired cell cycling capacity and reduced phospho-Rb levels observed in *p75[NTR]*-transduced HUVEC. PTTG1 was also reported to positively modulate angiogenesis. [36,47]

Illumina technology-based analysis of *p75[NTR]*-transduced murine muscles followed by real-time PCR of cultured HUVEC has identified that *p75[NTR]* downregulates the mRNA expression of *ITGB1* and of the endothelial specific *VEZF1* transcription factor, *in vitro* and *in vivo*. Notably, we also found down-regulated *VEGF-A*, *ITGB1*, and *VEZF-1* in diabetic muscles, which in part confirms previous reports of VEGF-A reduction as cause of diabetes-induced impaired neovascularization in skeletal muscles and myocardium.[1,4,48,49] Reduction in *ITGB1* content may be explained by the *p75[NTR]*-induced decrease in VEGF-A. In fact, in microvascular EC, VEGF-A upregulates the mRNA expression and activity of alpha(6)beta(1) integrin, which in turn mediates VEGF-A driven angiogenesis.[50] VEGF-A additionally binds to alpha(9)beta(1) integrin and this interaction is also essential for VEGF-A induced angiogenesis.[51] In line with this observation, *VEGF-A* rescued *ITGB1* level in *p75[NTR]*-HUVEC, once again suggesting that VEGF-A down-regulation plays an important role in orchestrating the molecular changes triggered by *p75[NTR]* in EC. The only outsider to this VEGF-A-based network seems to be *VEZF1*, whose impaired mRNA content was not corrected

by *VEGF-A* in *p75^NTR*-HUVEC. VEZF1 is a relatively scarcely explored transcription factor that was implicated in *in utero* vasculogenesis, post-natal angiogenesis, and EC survival.[52-54] Our expressional data discount the control of VEZF1 by VEGF-A. It is also improbable that VEZF-1 lies upstream of VEGF-A, because the anti-angiogenic effect caused by knocking down *VEZF1* expression was reportedly not corrected in the presence of VEGF-A.[54] Further studies are necessary to define the role of decreased VEZF1 in diabetes-induced microvascular complications. Our interpretation of the coordinated changes induced by *p75^NTR* in the molecular program of EC is summarized in Figure 3h. Because the importance of VEGF-A for the survival of neural cells has been established,[55] VEGF-A reduction may be also involved in p75^NTR-induced apoptosis of neural cells.[56] This hypothesis should be validated by future studies.

We finally conclude that *p75^NTR* over-expression is sufficient and necessary for altering angiogenesis in diabetes and becomes an obligatory target for therapy.

Methods

Cell cultures

HUVEC and MVEC were purchased from Cambrex (Belgium) and grown in EGM-2 medium (EBM-2 supplemented with EGM-2 SingleQuots, Cambrex) containing 5% FBS (Cambrex). HUVEC and MVEC were used between the second and the fifth passage in culture. Human endothelial progenitor cells (EPC) were enriched from peripheral blood of healthy volunteers: peripheral blood mononuclear cells (PB-MNC) were separated by density-gradient centrifugation (Histopaque 1077, Sigma), washed in phosphate buffered saline (PBS) and plated on fibronectin (10μg/ml, Sigma)-coated tissue culture plates in the EPC medium EGM-2MV (EBM-2 MV supplemented by EGM-2 MV SingleQuots, Cambrex) containing 10% FBS at a density of 1×10^6 MNC per cm^2. At day 4, non-adherent cells were removed and the adherent EPC were used for experiments.

Adenoviruses (*Ad*)

In order to prepare *Ad. p75^NTR*, the complete coding sequence of human *p75^NTR* was excised using EcoRI from a Bluescript plasmid (generous gift from Prof. Dario Marchetti, Louisiana State University, USA) and cloned in the adenovirus shuttle vector pDC515 (Microbix Biosystems, Canada) downstream of the mouse cytomegalovirus promoter. Replication-deficient adenoviruses were generated by site-specific FLP-mediated recombination of the cotransfected shuttle and genomic plasmids in 293 cells. Viral stocks were amplified, CsCl banded, and titrated as previously described.[57] To add a C-terminal V5 tag, the complete coding sequence of *p75^NTR* was amplified using KOD proofreading DNA polymerase (Novagen) to remove the stop codon. A perfect clone was excised and subcloned in a pDC515 shuttle vector containing the coding sequence of the V5 tag ready for adenovirus generation. Adenoviral vectors carrying human *p75^NTR* (*Ad. p75^NTR*) with or without a V5-tag were prepared. *Ad-rad66* (empty vector, also called *Ad.Null*) was used as negative control. To prepare the Ad.DN-*p75^NTR*, the regions containing the extracellular and transmembrane domains of rat *p75^NTR* was subjected to PCR and cloned into TrackCMV vector and subsequently sequenced for any PCR errors. The recombinant adenovirus was generated using bacterial recombination according to He *et al*[58] A high titer virus was produced using CsCl gradients and the CsCl was removed by dialysis. *Ad.VEGF-A* and *Ad.Myr-Akt* expressing a constitutively active mutant form of Akt were previously used by us.[12,26]

in vitro gene transfer

In order to infect HUVEC, MVEC, or human EPC, *Ad.VEGF-A* and its control *Ad.Null* was used at 10 M.O.I. *Ad.Myr-Akt* and its control *Ad.Null* was used at 100 M.O.I. The other Ads were used at 100 to 500 M.O.I.

Western-Blot analyses

Proteins were extracted from cultured cells, muscles, or BM by using ice-cold buffer A (50mM Hepes, 150mM NaCl, 1mM EDTA, 1mM EGTA, 25mM NaF, 5mM NaPPi, 1%Triton, 1% NP40, 1 mM Na_3VO_4, 0,25% sodium deoxycholate, 0.5mM Na-orthovanadate, 1 mM benzamidine, 0.1mM phenylmethylsulfonyl fluoride) or ice-cold RIPA buffer. Protein concentration was determined using the Bio-Rad Protein Assay Reagent (Bio-Rad). Detection of proteins by Western blot analysis was done following separation of whole cell extracts (50μg) on SDS-polyacrylamide gels. Proteins were transferred to polyvinylidene difluoride membranes (PVDF, Amersham-Pharmacia) and probed with the following antibodies: anti mouse p75[NTR] (clone ME20.4, Upstate Biotechnology, 1:1000), Ser 1177-phospho-eNOS (Cell Signaling, 1:1000), eNOS (Santa Cruz Biotechnology, 1:500), VEGF-A (Santa Cruz Biotechnology, 1:2000), Ser473-phospho-Akt (Cell Signaling, 1:1000), Akt (Cell Signaling, 1:1000), phospho-Rb (Upstate Biotechnology, 1:500), p-FAK (pY397, Transduction Laboratories, 1:1000), cleaved-caspase-3 (Cell Signaling, 1:1000), V5 (Novus Biological, 1:1000). GADPH (R&D System, 1:2000) was used as loading control. For detection, secondary antibody goat anti rabbit or anti mouse conjugated to horseradish peroxidase (Amersham Pharmacia, 1:5000) were used, followed by chemiluminescence reaction (ECL, Amersham Pharmacia).

FACS analysis of HUVEC for p75[NTR], Annexin-V, and PI

Surface antigen expression by HUVEC was analyzed by flow cytometry using combinations of phycoerythrin (PE)-conjugated mouse anti-human p75[NTR] and FITC-conjugated Annexin-V antibodies (both from BD Bioscience Pharmigen (BD)). Cells were also stained with PI. Unstained and single staining controls were performed to define positivity. Data were obtained on a FACS Calibur flow cytometer (BD) and analyzed using WinMDI (Purdue University, West Lafayette, USA). Cell numbers are expressed as percent of HUVEC. The experiment was performed in triplicate and repeated 3 times.

Caspase-Glo assay

HUVEC (7×10^3/well) and EPC (3×10^4/well) were seeded in flat bottomed 96-well plates and infected with *Ad.Null* or *Ad.p75[NTR]* (each at 100, 250, and 500 M.O.I.). Caspase-3 activity was measured by using a luminescent cell death detection kit (Caspase-Glo Assay, Promega), according to the instruction of the manufacturer. The apoptosis inducer staurosporin (1μM, for 4h) was used as a positive control of apoptotic death. The Caspase-Glo assay was also used to assess the effect of proNGF (5ng/mL, a concentration which was found to induce apoptosis of p75[NTR]-expressing EC,[17] Alomone), NGF (100ng/mL, Upstate), BDNF (100ng/mL, Upstate), soluble trkB receptor (used at 4ng/mL to block endogenous BDNF activity, R&D Systems), [17] and a goat-raised NGF neutralizing antibody (kindly donated by Dr. Luigi Aloe, CNR, Rome, Italy).[3,19] PBS and 0.01% non immune goat serum were used for controls in these experiements.[19] Each experiment was performed in triplicate and repeated at least 3 times.

TUNEL apoptosis assay of HUVEC and EPC

HUVEC or EPC were seeded (1.5×10^4/well) on gelatine and fibronectin-coated Labtek™ slides (Nalge Nunc Int.) and infected with *Ad.Null* or *Ad.p75[NTR]* overnight. After 48h, cells were fixed with 4% paraformaldehyde. TUNEL assay was performed according to the manufacturer's instructions (Calbiochem). Nuclei were counterstained with DAPI. At least 500

cells (in eight randomly captured microscopic fields at 400× magnification) were scored in a blinded fashion to calculate the percentage of TUNEL-positive nuclei. Data are expressed as the average percentage of apoptotic nuclei. The experiment was performed in triplicate and repeated 3 times.

Flow cytometry analysis of apoptotic microparticles

Endothelial microparticles (EMP) were collected from the conditioned culture medium of HUVEC by two centrifugation steps (1500 × g for 15 min, followed by 20500 × g for 5 min) and stored and at -80°C. Then, EMP were numbered by flow cytometry analysis as AnnexinV-positive microparticles, as described.[59] Analyses were performed using PE-conjugated mouse anti-human p75[NTR] antibody and its corresponding isotype control provided by BD. EMP (20μL) were incubated with 20μL of antibody for 30min in the dark. EMP were then analysed on a Beckman-Coulter EPICS XL flow cytometer in the presence of Flowcount calibrator beads. EMP gate was defined as events with a 0.1-1μm diameter and examined on a fluorescence/forward light scatter plot. The experiment was repeated 3 times.

Cell cycle analysis

HUVEC were infected with *Ad.p75^NTR* or *Ad.Null* (150 M.O.I.) and then synchronized by serum deprivation (0.1% FBS) for 16h. Next, cells were washed twice with PBS, released in complete medium, and harvested at different time points (indicated in Fig. 2a). After fixation in 70% ethanol and RNase A (100μg/ml, Sigma) treatment for 1h at 37°C, cells were stained with PI (50μg/ml, Sigma) on ice in the dark for 30min. DNA content was analyzed by flow cytometric analysis (Becton Dickinson FACScan, San Jose California) and quantification was performed by using the software Modfit LT for MAC version 2.0 (from Verity Software house, Topsham, Maine, USA). The experiment was repeated 3 times.

BrdU incorporation

HUVEC ($5×10^3$/well) were seeded in a 96-well plate and infected overnight (in EBM2 supplemented with 0.1% FBS) with *Ad.Null* or *Ad.p75^NTR* (250 M.O.I.). Then, the medium was replaced with complete EGM2 added with BrdU (10μM) for 24h. BrdU incorporation by HUVEC was measured by using a BrdU immunofluorescence assay kit from Roche, according to the manufacturer's instructions. Briefly, HUVEC were fixed and made permeable with FixDenat solution for 1h, then incubated with monoclonal anti-BrdU peroxidase-conjugated antibody (anti-BrdU-POD) for 90min. Bound anti-BrdU-POD was detected by a substrate reaction, then quantified by an ELISA plate reader. Each experiment was performed using 6 wells per group and repeated 3 times.

EPC were plated in a 6-well plate and infected with *Ad.Null* or *Ad. p75^NTR* (500 M.O.I.) in EBM2 with 0.1% FBS overnight. Then, the medium was changed in complete EGM2 containing BrdU (10μM) for 72h and the incorporation of BrdU by EPC was measured by FACS. Briefly, EPC were trypsinized, washed with PBS, and fixed with 70% ethanol on ice for 30min. Then, DNA was denatured in 2N HCl with 0.5% Triton X-100 for 30min at room temperature and neutralized in 0.1M $Na_2B_4O_7$, pH 8.5. Cells were finally incubated with monoclonal anti-BrdU antibody (Dako, 1:100) for 1h at room temperature, centrifuged, washed, stained with FITC-conjugated secondary for 30min and read at a FACS Calibur (Becton Dickinson). Evaluation was performed blind. Data were analyzed using CellQuest software (Becton Dickinson). Each experiment was performed in triplicates and repeated 3 times.

Migration assay

The migratory function of $p75^{NTR}$ or *Null*-transduced HUVEC and EPC was evaluated (at 12h and 48h from gene transfer) by using fibronectin-coated (10μg/ml, Sigma) 24-well-plate transwell migration inserts (Corning, Artington, UK) with a polycarbonate membrane of 8-μm (HUVEC) or 5-μm (EPC) pore size. Briefly, cells were trypsinized and resuspended in EBM-2 containing 0.1% bovine serum albumin (BSA, Sigma). Cells (0.5×10^5) were placed in the upper chamber, while EBM-2 containing 0.1% BSA and human recombinant SDF-1 (100ng/mL) was placed in the lower chamber. To control for spontaneous migration (negative control), EBM-2 with 0.1% BSA was used in the lower chamber. Cells were incubated in a humidified incubator at 37°C for 5h (HUVEC) or overnight (EPC). Non-migrated cells were removed by gently wiping the upper surface of the membrane with a cotton swab. Membranes were fixed in methanol, excised with a scalpel and mounted on microscope slides with mounting medium containing DAPI (Vectashield, Vector Technologies). Level of migration was assessed by counting the number of cells present on the lower surface of the membrane in 8 randomly captured fluorescence microscopic view fields (magnification 200X). Evaluation was performed blind. Each experiment was performed in triplicate and repeated 3 times.

Adhesion assay

Ninety-six-well tissue culture plates were coated for 1h with fibronectin (10μg/ml in PBS) and then blocked for 1h at 37°C with 1% BSA in PBS and washed 3 times with PBS before cell seeding. At 12h and 48h from infection with *Ad.p75^{NTR}* or *Ad.Null* (250 M.O.I. for HUVEC, 500 M.O.I. for EPC), transduced HUVEC (15×10^3/well) or EPC (20×10^3/well) were seeded in EGM2 with 10% FCS and incubated at 37°C. One hour later, non-adherent cells were discarded by washing 3 times and adherent cells were fixed (10 % formalin in PBS, pH 7.4 for 10min at room temperature) and stained with DAPI (2.5μg/ml, Sigma,) for 10min in the dark. Plates were then rinsed extensively with water and cell adhesion was quantified by counting adherent cells (magnification 200×). Evaluation was performed blind. Each experiment was performed in triplicate and repeated 3 times.

Matrigel assay

HUVEC (10^5 cell/well) were infected with *Ad.p75^{NTR}* or *Ad.Null* (250 M.O.I.) and, after 12h or 24h, seeded in 24-well plates coated with 300 μL of Matrigel supplemented with growth factors (Becton Dickinson). For rescue experiments with *VEGF-A* and *Myr-Akt*, cells were co-infected with *Ad.p75^{NTR}* or *Ad.Null* (250 M.O.I.) plus either 10 M.O.I. of *Ad.VEGF-A* or its control *Ad.Null* or 100 M.O.I. of *Ad.Myr-Akt* or its control *Ad.Null*. Plates were incubated at 37°C and photographed at different times from seeding. Capillary-like structure formation was examined under an inverted phase photomicroscope. Tube formation was quantified by counting the number of intersection points in randomly captured microscopic fields and/or by calculating the % microscopic field area covered by connected tubular structures (magnification 100×). Evaluation was performed blind. Each experiment was performed in triplicate and repeated 3 times.

NO generation assay

NO generation was assessed in $p75^{NTR}$-HUVEC and *Null*-HUVEC. Briefly, transduced HUVEC were detached by trypsinization and divided into four groups with n=4 replicates containing 2×10^5 cells. Samples were pre-incubated in sample buffer (200 mM Tris-HCl, 10mM CaCl2, 10mM MgCl2, 1.33mM NaCl, 65mM KCl, 5mM D-glucose, 0.1% BSA and 50μM L-arginine (all Sigma). To the $p75^{NTR}$L-NIO and *Null*L-NIO groups, the NOS inhibitor L-N5-(1-Iminoethyl)ornithine (L-NIO, 100μM, Merck, UK) was added for 10min whereas the other two groups remained without inhibitor. DAF-2DA (5μM; Invitrogen, UK) was added to all samples and incubated in the dark for 3h at 37°C. Cells were washed with sample buffer

and immediately FL1 fluorescence was determined in a FACS Calibur flow cytometer (BD). FL1 mean fluorescence intensity was calculated and unspecific fluorescence remaining after NOS inhibition by L-NIO was subtracted from uninhibited FL1 fluorescence intensity to obtain NOS specific DAF fluorescence values reflecting NO generation.

Gene transfer to murine muscles

Anaesthetized mice received 3 adenovirus injections (for a total of 10^9 p.f.u. virus in 20μL) into 3 equidistant sites of the normoperfused or ischemic left adductor muscles. When desired, ischemia was induced (*vide infra*) immediately before gene transfer.

Illumina beadarray gene expression profiling

RNA samples from *Null* and *p75^NTR* infected murine muscle were amplified and biotinylated using the Illumina TotalPrep RNA amplification Kit (Ambion, Austin, TX). Eight samples that passed quality control were randomly allocated to Sentrix Mouse-6 Expression bead chip arrays (Illumina, San Diego, CA), interrogating 46,600 transcripts from the mouse genome. Samples were hybridized to the beadchip arrays, followed by scanning and feature extraction, all performed at ServiceXS (Leiden, The Netherlands). Array data were extracted using Illumina BeadStudio software. Normalization and statistical analysis of the bead summary data from the arrays was carried out using the limma package 5 in R/Bioconductor (www.bioconductor.org). Bead summary intensities were normalized using quantile normalization and differential expression between the treatments of interest was assessed using a moderated t-test.[60] This test is similar to a standard t-test for each probe except that the standard errors are moderated across genes to ensure more stable inference for each gene using Baysian statistics. Genes were considered significant if the P values, adjusted for multiple testing by using Benjamini and Hochberg's method,[61] were <0.05. The false discovery rate was thereby controlled to be <5%. Differential modulation of specific pathways was assessed using the Panther-annotated protein group expression statistical analysis.[62] Micro-array expression data are available at the NCBI Gene Expression Omnibus (GEO) (http://www.ncbi.nlm.nih.gov/project/geo) under accession number GSE9910.

GEArray

Human GEArray kit (SuperArray Inc., Bethesda, MD, USA), composed of 113 genes connected to the p53 signaling pathway and two housekeeping genes (actin and GADPH), was used to characterize gene expression profile of HUVEC cells infected with *Ad.p75^NTR* or *Ad.Nul* (250 M.O.I.). Total RNA was isolated from cells by RNeasy isolation kit (Qiagen, Crawley, UK). cRNA probes for array analysis were synthesized following the manufacturer's directions. Differential gene expression patterns were detected by autoradiography. The experiment was performed in triplicate and data were confirmed by real-time quantitative PCR.

Real-time quantitative RT-PCR

Total RNA was isolated from HUVEC and murine muscles (RNeasy, Qiagen, UK) and RNA quality confirmed using the RNA Nano LabChip in a bioanalyzer (Agilent). RNA was reverse transcribed (Sensiscript reverse transcriptase, Qiagen) and quantitative PCR was performed in a LightCycler (Roche, Burgess Hill, UK) using the following primers: 18s rRNA (forward: 5′- TAGAGGGACAAGTGGCGTTC -3′, reverse: 5′- TGTACAAAGGGCAGGGACTT- 3′), murine *VEGF-A* (forward: GGAGATCCTTCGAGGAGCACTT, reverse: GGCGATTTAGCAGCAGATATAAGAA), human *VEGF-A* (forward: CTACCTCCACCATGCCAAGTG, reverse: GATGATTCTGCCCTCCTCCTT), human *BIRC5* (forward: TCCGGTTGCGCTTTCCT, reverse: TCTTCTTATTGTTGGTTTCCTT), human *PTTG1* (forward: CGGCTGTTAAGACCTGCAATA, reverse: TTCAGCCCATCCTTAGCAACC), mouse *ITGB1* (forward:

CGTGGTTGCCGGAATTGTTC, reverse: ACCAGCTTTACGTCCATAGTTTG), human *ITGB1* (forward: AAGCTTTTAATGATAATTCATGACAG, reverse: GCCACTTTGCTTTTTGGATG), murine *VEZF1* (forward: CAGCAGCCGAACTTCGTTG, reverse: CAGGCTTACTGGGTTTCTTGAC), human *VEZF1* (forward: GACAGCAGCCGAACTTCGTT, reverse: TGCCCGAGGAAGATGTAGTGA), human *p75^NTR* (forward: GTGGGCCTTGTGGCCTAC, reverse: TGTGGCCTACATAGCCTTC). The analyses were performed on at least 4 samples per time and repeated three times.

Limb ischemia and diabetes models

Left limb ischemia was induced in anaesthetized CD1 male mice, as described.[3,9,12,41] Type-1 diabetes was induced by streptozotocin, as also described.[63] Diabetic mice did not received insulin and were studied between 1 and 3 months from diabetes onset. In all experiments, normoglycemic controls were age-and gender-matched.

Clinical outcome from ischemia and BF measurements

Following limb ischemia induction, we evaluated the toe and foot necrosis event, as described.[9,10,41] Superficial BF of the ischemic and contralateral foot was analyzed at different time-points from ischemia induction by color laser Doppler (Lisca Perimed, Sweden) and the ratio between BF in the ischemic foot and BF in controlateral foot was calculated and used as an index of % BF recovery.[3,9,10,12,41] Intra-muscular BF was measured by Oxylite/Oxyflow (Oxford Optronic, Oxford, UK) by inserting a probe in the adductor muscle of anaesthetized mice.[26] The number of auto-amputated or necrotic fingers in the ischemic foot was calculated, as previously explained.[9,41] A minimum of n=12 mice per group were studied.

Capillary density

Capillary density was determined on H&E-stained transverse sections of adductor muscles (observed at 1000X magnification) by the aid of an ocular graticule, as previously described.[3,9,10,12,41] and in fluorescent sections stained for isolectin B4 (red fluorescence) (Molecular Porbes) to identify EC and with DAPI (blue fluorescence) (Sigma Aldrich) to identify nuclei. A minimum of n=6 muscles per each group were used for these analyses.

Apoptosis and proliferation in muscles

Apoptosis was recognized by TUNEL assay, as previously described.[3,9,10,12,41] Cell proliferation was recognized by IHC for either the proliferation cell nuclear antigen (PCNA) or the mini-chromosome maintenance protein 2 (MCM2), a marker of cycling cells, as also previously published.[26,42] Additional sections were triple stained for either TUNEL, isolectin B4, and DAPI or PCNA, isolectin B4, and DAPI. A minimum of n=6 muscles per each group were used for these analyses.

Other immunohistochemical analyses of muscular sections

Following the delivery of V5-tagged *Ad.p75^NTR* to adductor muscles, transgene expression by capillary EC was evaluated by staining paraffin-embedded adductor sections with a FITC-conjugated primary antibody recognizing V5 (Novus Biological, 1:200) and EC by Alexa 568-conjugated isolectinB4 (Molecular Probe, 1:200). In a separate experiment, expression of endogenous mouse p75^NTR by EC was analyzed by co-staining adductor sections with a FITC-conjugated primary antibody recognizing mouse p75^NTR (Calbiochem, 1:200)and Alexa 568-conjugated isolectinB4.

FACS analyses of bone marrow

BM-MNC were obtained from the left leg of freshly killed CD1 mice, as described previously.[64] Briefly, tibiae and femora were flushed with DMEM (Cambrex) containing 5% FCS (Biochrom, Berlin, Germany). Cells were separated and passed through a 70μm cell strainer (BD, Oxford, UK). Single cell suspensions were centrifuged on Histopaque 1083 (Sigma) to obtain MNC. Surface antigen expression of MNC was analyzed by flow cytometry using combinations of PE-labelled anti-Sca-1 (BD), FITC-labelled anti-lineage markers-Alexa 488 (Caltag), FITC-labelled or biotinylated Annexin-V (BD), and Cy5 labeled-p75[NTR] (Advance Targeting System, CA, USA) together with PE- or FITC-labelled anti-rabbit secondary antibody (Sigma Aldrich) (all monoclonal). Unstained and staining controls for single colors and secondary antibodies were performed to define positivity. Data were obtained on a FACS Calibur flow cytometer (BD) and analyzed using WinMDI (Purdue University, West Lafayette, USA). Cell numbers are expressed as percent of a sub-population as specified. A minimum of n=6 mice per group were used for these analyses.

FACS for GFP fluorescence of BM cells

Anaesthetized normoglycemic and diabetic mice received 3 injections of *Ad.GFP* (for a total of 10^9 p.f.u. in 20μL) into 3 equidistant sites of the ischemic left adductor muscles. After 3d, BM-MNC were obtained from both legs of freshly killed CD1 mice. The presence of green fluorescent BM-MNC was determined by FACS Calibur flow cytometer (BD). A minimum of n=5 mice per group were used for these analyses.

Statistical analysis

All results are expressed as the mean±SEM. Statistical analysis was performed via a t-test when two groups were analyzed, or via an ANOVA, followed by a Bonferroni post hoc test for multiple comparisons. A P value of <0.05 was taken as statistically significant. The statistical analysis used for Illumina data is described above.

Supplementary Material

Refer to Web version on PubMed Central for supplementary material.
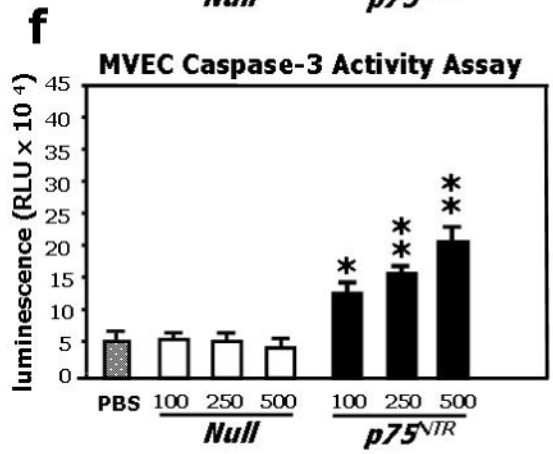
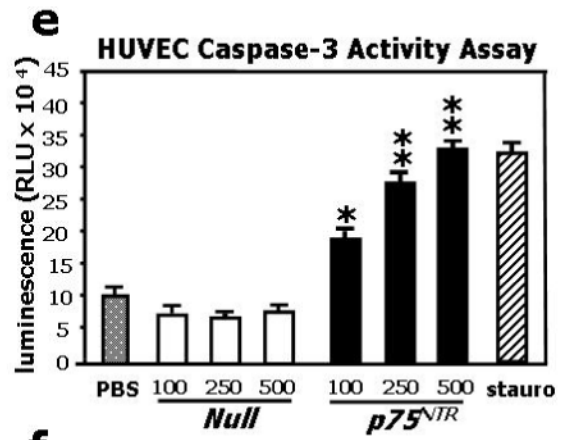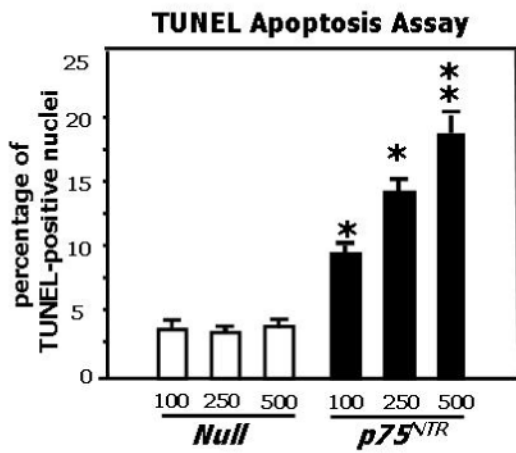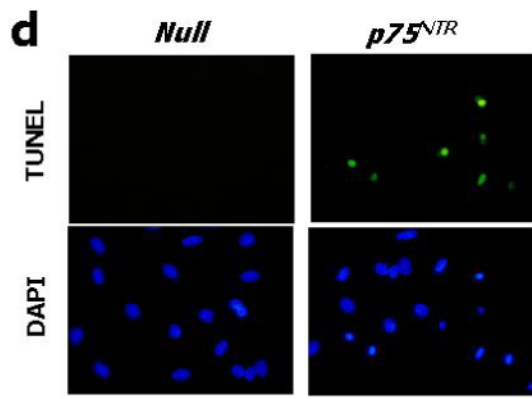## Acknowledgements

Bibliography

1. Yoon YS, et al. Progressive attenuation of myocardial vascular endothelial growth factor expression is a seminal event in diabetic cardiomyopathy: restoration of microvascular homeostasis and recovery of cardiac function in diabetic cardiomyopathy after replenishment of local vascular endothelial growth factor. Circulation 2005;111:2073–85. [PubMed: 15851615]

2. Tepper OM, et al. Human endothelial progenitor cells from type II diabetics exhibit impaired proliferation, adhesion, and incorporation into vascular structures. Circulation 2002;106:2781–6. [PubMed: 12451003]

3. Salis MB, et al. Nerve growth factor supplementation reverses the impairment, induced by Type 1 diabetes, of hindlimb post-ischaemic recovery in mice. Diabetologia 2004;47:1055–63. [PubMed: 15184980]

4. Rivard A, et al. Rescue of diabetes-related impairment of angiogenesis by intramuscular gene therapy with adeno-VEGF. Am J Pathol 1999;154:355–63. [PubMed: 10027394]

5. Loomans CJ, et al. Endothelial progenitor cell dysfunction: a novel concept in the pathogenesis of vascular complications of type 1 diabetes. Diabetes 2004;53:195–9. [PubMed: 14693715]

6. Krankel N, et al. Hyperglycemia reduces survival and impairs function of circulating blood-derived progenitor cells. Arterioscler Thromb Vasc Biol 2005;25:698–703. [PubMed: 15662022]

7. Ingram DA, et al. In Vitro Hyperglycemia or a Diabetic Intrauterine Environment Reduces Neonatal Endothelial Colony Forming Cell Numbers and Function. Diabetes. 2007

8. Gallagher KA, et al. Diabetic impairments in NO-mediated endothelial progenitor cell mobilization and homing are reversed by hyperoxia and SDF-1 alpha. J Clin Invest 2007;117:1249–59. [PubMed: 17476357]

9. Gadau S, et al. Benfotiamine accelerates the healing of ischaemic diabetic limbs in mice through protein kinase B/Akt-mediated potentiation of angiogenesis and inhibition of apoptosis. Diabetologia 2006;49:405–20. [PubMed: 16416271]

10. Emanueli C, et al. Nitropravastatin stimulates reparative neovascularisation and improves recovery from limb Ischaemia in type-1 diabetic mice. Br J Pharmacol 2007;150:873–82. [PubMed: 17351667]

11. Emanueli C, et al. Prophylactic gene therapy with human tissue kallikrein ameliorates limb ischemia recovery in type 1 diabetic mice. Diabetes 2004;53:1096–103. [PubMed: 15047627]

12. Emanueli C, et al. Type-2 diabetic Lepr(db/db) mice show a defective microvascular phenotype under basal conditions and an impaired response to angiogenesis gene therapy in the setting of limb ischemia. Front Biosci 2007;12:2003–12. [PubMed: 17127438]

13. Brem H, Tomic-Canic M. Cellular and molecular basis of wound healing in diabetes. J Clin Invest 2007;117:1219–22. [PubMed: 17476353]

14. Jeffcoate WJ, Harding KG. Diabetic foot ulcers. Lancet 2003;361:1545–51. [PubMed: 12737879]

15. Emanueli C, et al. Nerve growth factor promotes angiogenesis and arteriogenesis in ischemic hindlimbs. Circulation 2002;106:2257–62. [PubMed: 12390957]

16. Cantarella G, et al. Nerve growth factor-endothelial cell interaction leads to angiogenesis in vitro and in vivo. Faseb J 2002;16:1307–9. [PubMed: 12154004]

17. Kim H, Li Q, Hempstead BL, Madri JA. Paracrine and autocrine functions of brain-derived neurotrophic factor (BDNF) and nerve growth factor (NGF) in brain-derived endothelial cells. J Biol Chem 2004;279:33538–46. [PubMed: 15169782]

18. Kermani P, et al. Neurotrophins promote revascularization by local recruitment of TrkB+ endothelial cells and systemic mobilization of hematopoietic progenitors. J Clin Invest 2005;115:653–63. [PubMed: 15765148]

19. Caporali A, et al. Identification of the prosurvival activity of nerve growth factor on cardiac myocytes. Cell Death Differ. 2007

20. Lopez-Sanchez N, Frade JM. Control of the cell cycle by neurotrophins: lessons from the p75 neurotrophin receptor. Histol Histopathol 2002;17:1227–37. [PubMed: 12371150]

21. Ibanez CF. Jekyll-Hyde neurotrophins: the story of proNGF. Trends Neurosci 2002;25:284–6. [PubMed: 12086739]

22. Reichardt LF. Neurotrophin-regulated signalling pathways. Philos Trans R Soc Lond B Biol Sci 2006;361:1545–64. [PubMed: 16939974]

23. Lee R, Kermani P, Teng KK, Hempstead BL. Regulation of cell survival by secreted proneurotrophins. Science 2001;294:1945–8. [PubMed: 11729324]

24. Nykjaer A, et al. Sortilin is essential for proNGF-induced neuronal cell death. Nature 2004;427:843–8. [PubMed: 14985763]

25. Kenchappa RS, et al. Ligand-dependent cleavage of the P75 neurotrophin receptor is necessary for NRIF nuclear translocation and apoptosis in sympathetic neurons. Neuron 2006;50:219–32. [PubMed: 16630834]

26. Emanueli C, et al. Akt/protein kinase B and endothelial nitric oxide synthase mediate muscular neovascularization induced by tissue kallikrein gene transfer. Circulation 2004;110:1638–44. [PubMed: 15364809]

27. Boulanger CM, Amabile N, Tedgui A. Circulating microparticles: a potential prognostic marker for atherosclerotic vascular disease. Hypertension 2006;48:180–6. [PubMed: 16801490]

28. Koga H, et al. Elevated levels of VE-cadherin-positive endothelial microparticles in patients with type 2 diabetes mellitus and coronary artery disease. J Am Coll Cardiol 2005;45:1622–30. [PubMed: 15893178]

29. Tushuizen ME, et al. Elevated endothelial microparticles following consecutive meals are associated with vascular endothelial dysfunction in type 2 diabetes. Diabetes Care 2007;30:728–30. [PubMed: 17327351]

30. Knudsen ES, Wang JY. Differential regulation of retinoblastoma protein function by specific Cdk phosphorylation sites. J Biol Chem 1996;271:8313–20. [PubMed: 8626527]

31. Urbich C, et al. Soluble factors released by endothelial progenitor cells promote migration of endothelial cells and cardiac resident progenitor cells. J Mol Cell Cardiol 2005;39:733–42. [PubMed: 16199052]

32. Deshane J, et al. Stromal cell-derived factor 1 promotes angiogenesis via a heme oxygenase 1-dependent mechanism. J Exp Med 2007;204:605–18. [PubMed: 17339405]

33. Papapetropoulos A, Garcia-Cardena G, Madri JA, Sessa WC. Nitric oxide production contributes to the angiogenic properties of vascular endothelial growth factor in human endothelial cells. J Clin Invest 1997;100:3131–9. [PubMed: 9399960]

34. Angelucci A, Bologna M. Targeting vascular cell migration as a strategy for blocking angiogenesis: the central role of focal adhesion protein tyrosine kinase family. Curr Pharm Des 2007;13:2129–45. [PubMed: 17627545]

35. Papapetropoulos A, et al. Angiopoietin-1 inhibits endothelial cell apoptosis via the Akt/survivin pathway. J Biol Chem 2000;275:9102–5. [PubMed: 10734041]

36. Thompson AD 3rd, Kakar SS. Insulin and IGF-1 regulate the expression of the pituitary tumor transforming gene (PTTG) in breast tumor cells. FEBS Lett 2005;579:3195–200. [PubMed: 15922332]

37. Graiani G, et al. Nerve growth factor promotes reparative angiogenesis and inhibits endothelial apoptosis in cutaneous wounds of Type 1 diabetic mice. Diabetologia 2004;47:1047–54. [PubMed: 15164170]

38. Hochberg Y, Benjamini Y. More powerful procedures for multiple significance testing. Stat Med 1990;9:811–8. [PubMed: 2218183]

39. Chavakis E, et al. Role of beta2-integrins for homing and neovascularization capacity of endothelial progenitor cells. J Exp Med 2005;201:63–72. [PubMed: 15623573]

40. Sbaa E, et al. Caveolin plays a central role in endothelial progenitor cell mobilization and homing in SDF-1-driven postischemic vasculogenesis. Circ Res 2006;98:1219–27. [PubMed: 16601228]

41. Invernici G, et al. Human fetal aorta contains vascular progenitor cells capable of inducing vasculogenesis, angiogenesis, and myogenesis in vitro and in a murine model of peripheral ischemia. Am J Pathol 2007;170:1879–92. [PubMed: 17525256]

42. Graiani G, et al. Genetic deletion of the p66Shc adaptor protein protects from angiotensin II-induced myocardial damage. Hypertension 2005;46:433–40. [PubMed: 15998704]

43. Ackah E, et al. Akt1/protein kinase Balpha is critical for ischemic and VEGF-mediated angiogenesis. J Clin Invest 2005;115:2119–27. [PubMed: 16075056]

44. O'Connor DS, et al. Control of apoptosis during angiogenesis by survivin expression in endothelial cells. Am J Pathol 2000;156:393–8. [PubMed: 10666367]

45. Zwerts F, et al. Lack of endothelial cell survivin causes embryonic defects in angiogenesis, cardiogenesis, and neural tube closure. Blood 2007;109:4742–52. [PubMed: 17299096]

46. Suzuki A, et al. Survivin initiates cell cycle entry by the competitive interaction with Cdk4/p16 (INK4a) and Cdk2/cyclin E complex activation. Oncogene 2000;19:3225–34. [PubMed: 10918579]

47. Heaney AP, Horwitz GA, Wang Z, Singson R, Melmed S. Early involvement of estrogen-induced pituitary tumor transforming gene and fibroblast growth factor expression in prolactinoma pathogenesis. Nat Med 1999;5:1317–21. [PubMed: 10546001]

48. Boodhwani M, et al. Functional, cellular, and molecular characterization of the angiogenic response to chronic myocardial ischemia in diabetes. Circulation 2007;116:I31–7. [PubMed: 17846323]

49. Kivela R, et al. Effects of experimental type 1 diabetes and exercise training on angiogenic gene expression and capillarization in skeletal muscle. Faseb J 2006;20:1570–2. [PubMed: 16816123]

50. Lee TH, et al. Integrin regulation by vascular endothelial growth factor in human brain microvascular endothelial cells: role of alpha6beta1 integrin in angiogenesis. J Biol Chem 2006;281:40450–60. [PubMed: 17085437]

51. Vlahakis NE, et al. Integrin alpha9beta1 directly binds to vascular endothelial growth factor (VEGF)-A and contributes to VEGF-A-induced angiogenesis. J Biol Chem 2007;282:15187–96. [PubMed: 17363377]

52. Xiong JW, Leahy A, Lee HH, Stuhlmann H. Vezf1: A Zn finger transcription factor restricted to endothelial cells and their precursors. Dev Biol 1999;206:123–41. [PubMed: 9986727]

53. Kuhnert F, et al. Dosage-dependent requirement for mouse Vezf1 in vascular system development. Dev Biol 2005;283:140–56. [PubMed: 15882861]

54. Miyashita H, Kanemura M, Yamazaki T, Abe M, Sato Y. Vascular endothelial zinc finger 1 is involved in the regulation of angiogenesis: possible contribution of stathmin/OP18 as a downstream target gene. Arterioscler Thromb Vasc Biol 2004;24:878–84. [PubMed: 15031128]

55. Greenberg DA, Jin K. From angiogenesis to neuropathology. Nature 2005;438:954–9. [PubMed: 16355213]

56. Dechant G, Barde YA. The neurotrophin receptor p75(NTR): novel functions and implications for diseases of the nervous system. Nat Neurosci 2002;5:1131–6. [PubMed: 12404007]

57. Sala-Newby GB, Freeman NV, Curto MA, Newby AC. Metabolic and functional consequences of cytosolic 5′-nucleotidase-IA overexpression in neonatal rat cardiomyocytes. Am J Physiol Heart Circ Physiol 2003;285:H991–8. [PubMed: 12750059]

58. He TC, et al. A simplified system for generating recombinant adenoviruses. Proc Natl Acad Sci U S A 1998;95:2509–14. [PubMed: 9482916]

59. Leroyer AS, et al. Cellular origins and thrombogenic activity of microparticles isolated from human atherosclerotic plaques. J Am Coll Cardiol 2007;49:772–7. [PubMed: 17306706]

60. Baldi P, Long AD. A Bayesian framework for the analysis of microarray expression data: regularized t -test and statistical inferences of gene changes. Bioinformatics 2001;17:509–19. [PubMed: 11395427]

61. Thomas PD, et al. Applications for protein sequence-function evolution data: mRNA/protein expression analysis and coding SNP scoring tools. Nucleic Acids Res 2006;34:W645–50. [PubMed: 16912992]

62. Benjamini Y, H Y. Controlling the false discovery rate: a practical and powerful approach to multiple testing. Journal of the Royal Statistical Society 1995;57:289–300.

63. Emanueli C, et al. Prevention of diabetes-induced microangiopathy by human tissue kallikrein gene transfer. Circulation 2002;106:993–9. [PubMed: 12186806]

64. Madeddu P, et al. Phosphoinositide 3-Kinase {gamma} Gene Knockout Impairs Postischemic Neovascularization and Endothelial Progenitor Cell Functions. Arterioscler Thromb Vasc Biol. 2007
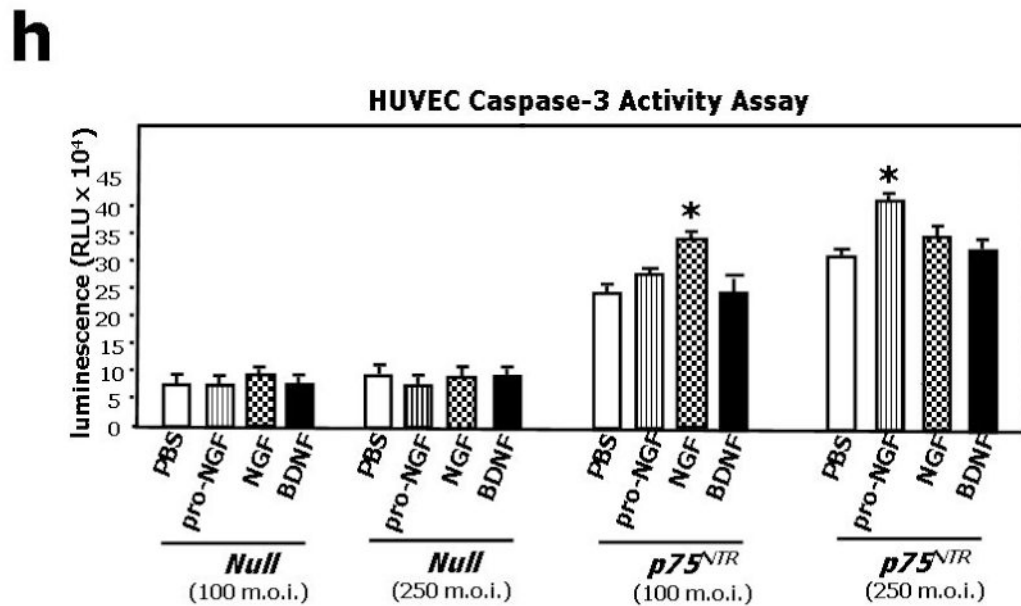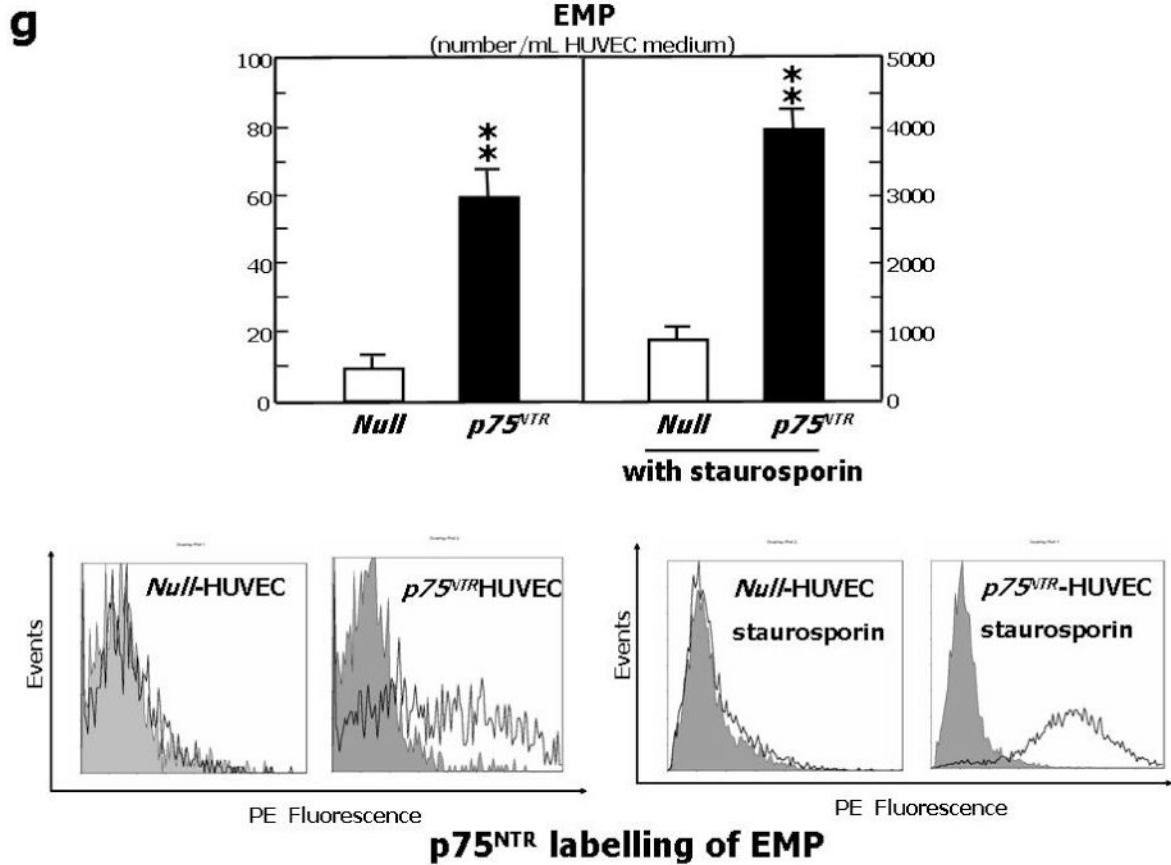
**g**

EMP
(number /mL HUVEC medium)

with staurosporin

Null-HUVEC   **p75^NTR HUVEC**   **Null-HUVEC staurosporin**   **p75^NTR-HUVEC staurosporin**

PE Fluorescence

p75^NTR labelling of EMP

h

HUVEC Caspase-3 Activity Assay

Null
(100 m.o.i.)   *Null*
(250 m.o.i.)   *p75^NTR*
(100 m.o.i.)   *p75^NTR*
(250 m.o.i.)
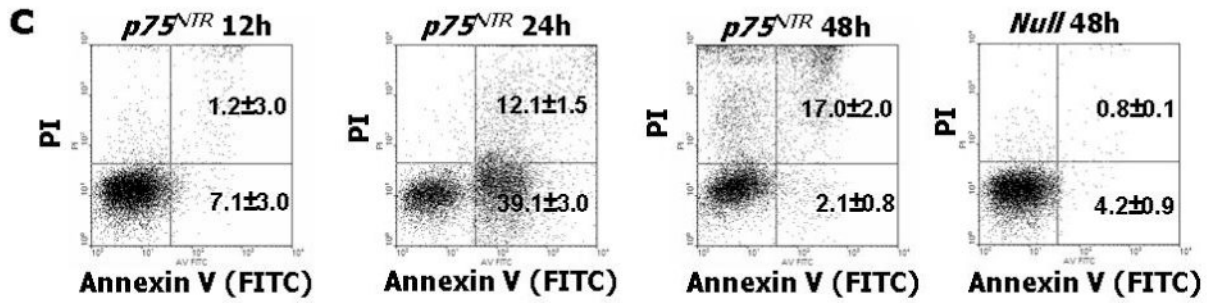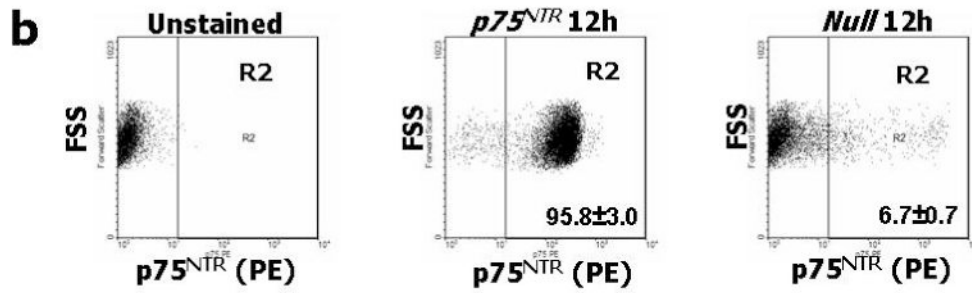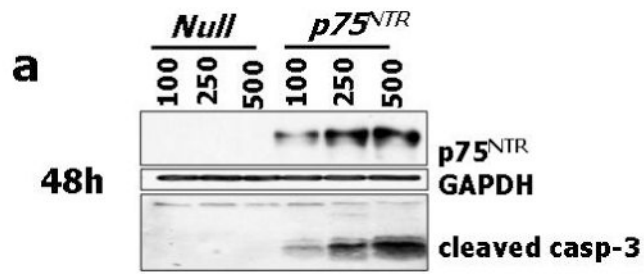
Fig. 1. Adenovirus-mediated p75^NTR transduction of EC promotes apoptosis *via* caspase-3 cleavage and stimulates the production of apoptotic microparticles from HUVEC
(a) HUVEC were infected with 100, 250 and 500 M.O.I. of *Ad.Null* or *Ad.p75^NTR*, as indicated. After 48h, cell lysates were collected and subjected to western blotting with antibodies to p75^NTR, cleaved caspase-3, and GAPDH (used as loading control). (**b**) FACS analyses for

p75^{NTR} show abundant receptor expression (95.8±3%) at 12h from gene transfer with
Ad.p75^{NTR} (250 M.O.I.), while at 12h from *Null* gene transfer, p75^{NTR}-expressing HUVEC
are only 6.7±0.7%. (**c**) p75^{NTR}-expressing HUVEC were gated and studied at 12h, 24h, and
48h for co-expression with Annexin-V and propidium iodide (PI) to detect apoptosis. This
analysis revealed that at 12h from *Ad.p75^{NTR}*, less than 9% of p75^{NTR}-carrying cells presented
Annexin-V on the external plasma membrane. Early apoptosis (cells positive for Annexin-V
and negative for PI, lower right squares) peaked at 24h (39.1±3% of p75^{NTR}-expressing
HUVEC), followed by late apoptosis (cells positive for both Annexin-V and PI, upper right
squares) at 48h from *Ad.p75^{NTR}* (17.05±2% of p75^{NTR}-expressing HUVEC). (**d**) HUVEC were
treated as described in (a) and apoptotic nuclei were detected by TUNEL assay. Fluorescent
images are representative of apoptosis rate in *Null*-HUVEC and *p75^{NTR}*-HUVEC. Bar graphs
quantify apoptosis, which is expressed as percentage of TUNEL-positive nuclei (green
fluorescence) to total nuclei (stained in blue fluorescence by DAPI). Data are presented as
means±SEM. *P<0.05 and **P<0.001 vs. *Ad.Null*. (**e,f**) Caspase-3 activity assay was
performed on HUVEC (e) or MVEC (f). Cells (5000 cells/well) were infected with 100, 250
or 500 M.O.I. of *Ad.Null* or *Ad.p75^{NTR}* or left uninfected (PBS). After 48h, Caspase-Glo 3/7
was incubated for 1h before recording luminescence. The apoptosis inducer staurosporin
(stauro, 1μM) was used as reference in (e). Values are means±SEM. *P<0.05 and **P<0.001
vs. *Ad.Null*. (**g**) Upper panel: Concentration of endothelial apoptotic microparticles (EMP)
released by *Null*-HUVEC or *p75^{NTR}*-HUVEC under no other stimulation or following
incubation with the apoptosis inducer staurosporin (100 nM, 16h). Values are means±SEM.
**P<0.01 vs. *Ad.Null*. Lower panel: p75^{NTR} is present in EMP released by HUVEC. The
shadow peak corresponds to fluorescence background obtained with the isotypic control of
p75^{NTR} antibody. The second peak represents the specific labelling of EMPs with fluorescent
p75^{NTR} antibody. (**h**) Caspase-3 activity assay performed on HUVEC infected with *Ad.Null*
or *Ad. p75^{NTR}* (each at 100 and 250 M.O.I.) before being treated with PBS, proNGF (5ng/mL),
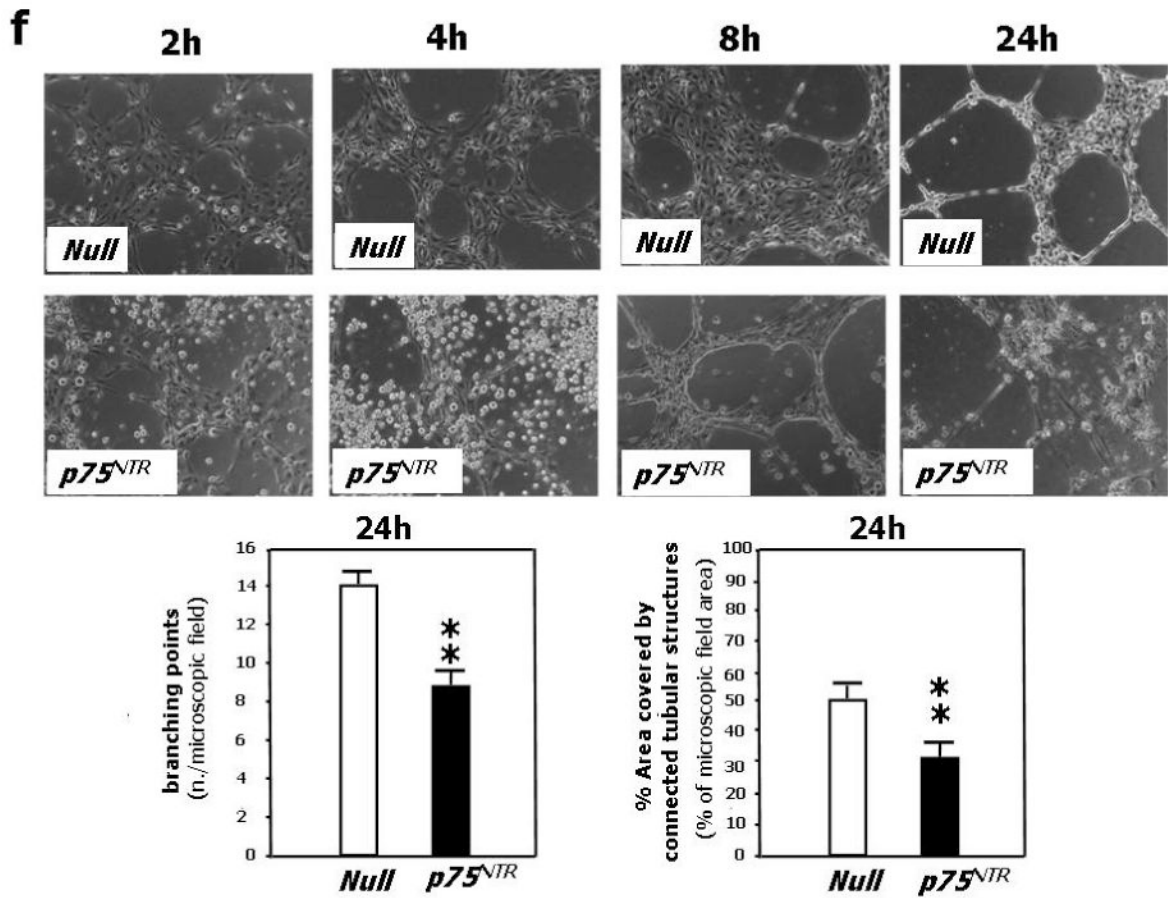NGF (100ng/mL), or BDNF (100ng/mL) for 24h. Values are means±SEM. *P<0.01 vs. PBS.
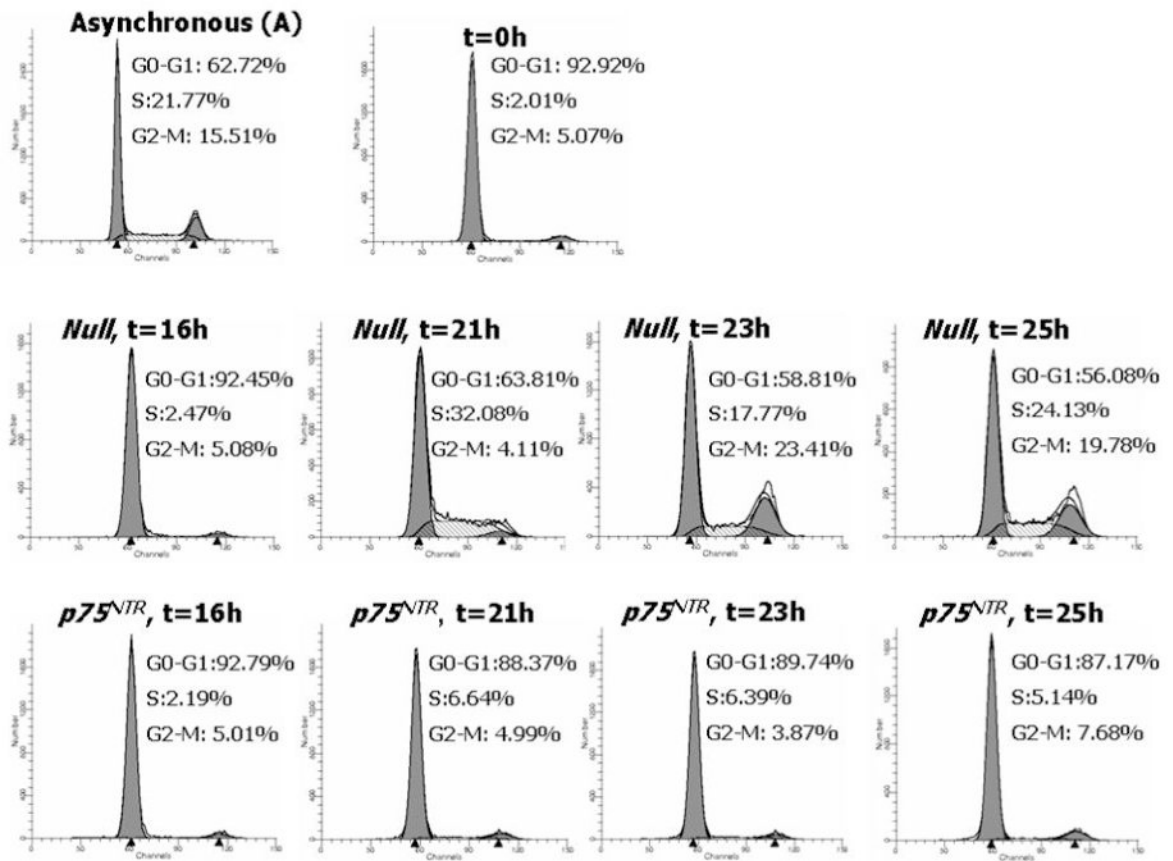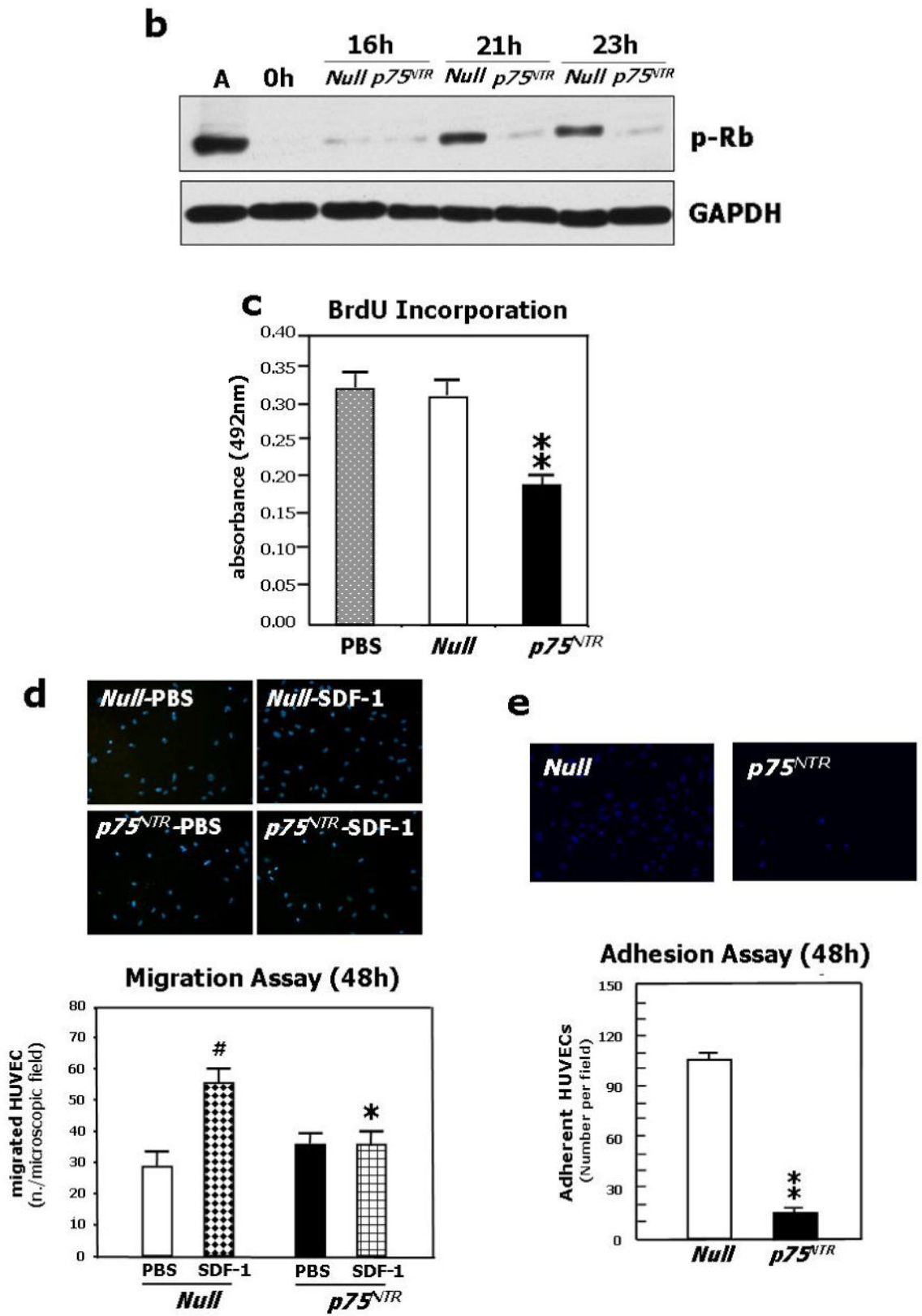
Fig. 2. p75^{NTR} inhibits EC cell cycle progression and impairs EC ability to proliferate, migrate, adhere, and form capillary-like tubular structures *in vitro*

(a) HUVEC were infected with either *Ad.Null* or *Ad.p75^{NTR}* (250 M.O.I.). Cells were synchronized by overnight serum starvation. After release, by flow cytometric analysis, cell cycle progression was assessed at the indicated time points. The percentage of cells in G1, S, and G2 phases is indicated in figures. **(b)** Western blot analysis of phosphorylated tumor suppressor retinoblastoma protein (p-Rb) (marker of cell cycle progression) on total cell extracts derived from HUVEC. GAPDH was used as loading control. **(c)** Proliferation (measured by BrdU incorporation) of HUVEC infected with *Ad.Null* or *Ad.p75^{NTR}* (250 M.O.I.) or uninfected (PBS). **P<0.01 vs. *Ad.Null*. **(d)** Migration toward SDF-1 (100ng/mL) or PBS (vehicle) of HUVEC infected 48h in advance with *Ad.p75^{NTR}* or *Ad.Null* (250 M.O.I.) In bar graph, values are means±SEM. #P<0.05 vs. *Ad.Null* combined with PBS, *P<0.05 vs. *Ad.Null* combined with SDF-1. Upper panels show representative microscopic fields (original magnification 200×) **(e)** Adhesion assay of HUVEC infected 48h earlier as in (d). HUVEC adhesion was quantified by counting adherent cells following washing of non adherent cells and DAPI staining of nuclei of adherent cells. In bar graph, values are means±SEM. **P<0.01 vs. *Ad.Null*. Upper panels show representative photomicrographs (magnification 200×) **(f)** Time-course (up to 24h from cell seeding) of tubular structure formation on matrigel. Twelve hours before being seeded on Matrigel-coated dishes, HUVEC were infected with *Ad.Null* or *Ad.p75^{NTR}*. In bar graph, the quantification of EC tube network formation at 24h from seeding is expressed as the number of intersecting points of tubular structures for microscopic field (left) as well as the % of microscopic field area covered by connected tubular structures (right).

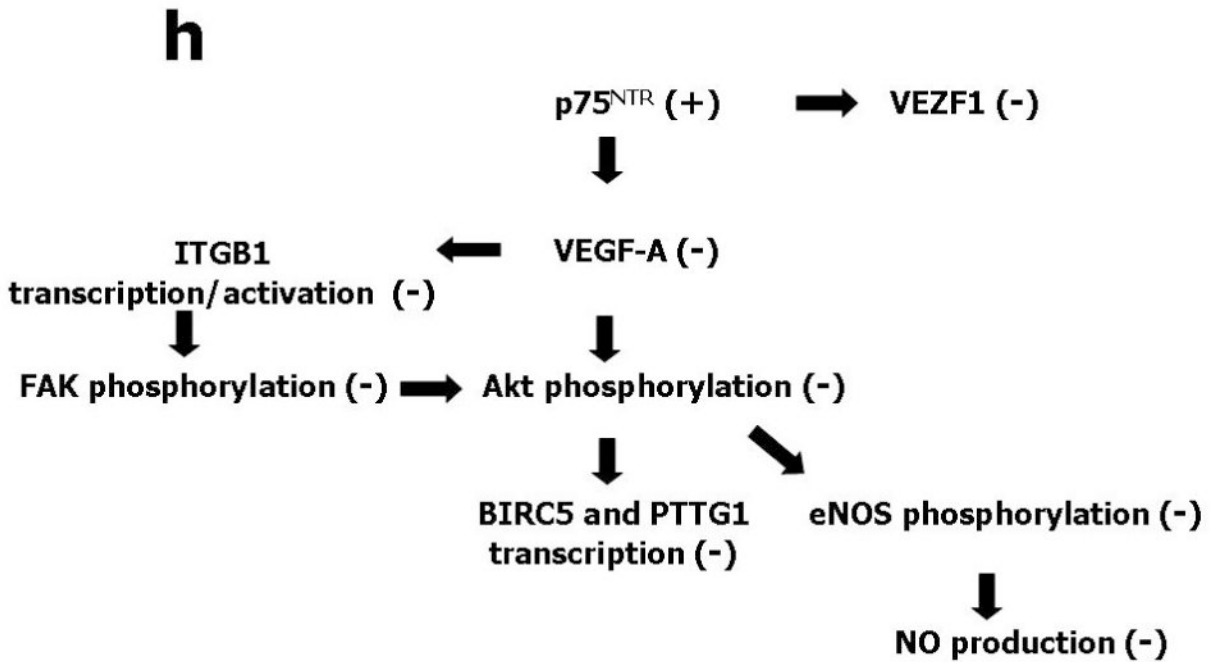Values are means±SEM. **P<0.01 vs. *Ad.Null.* Upper panel: show representative photomicrographs (original magnification 100×).
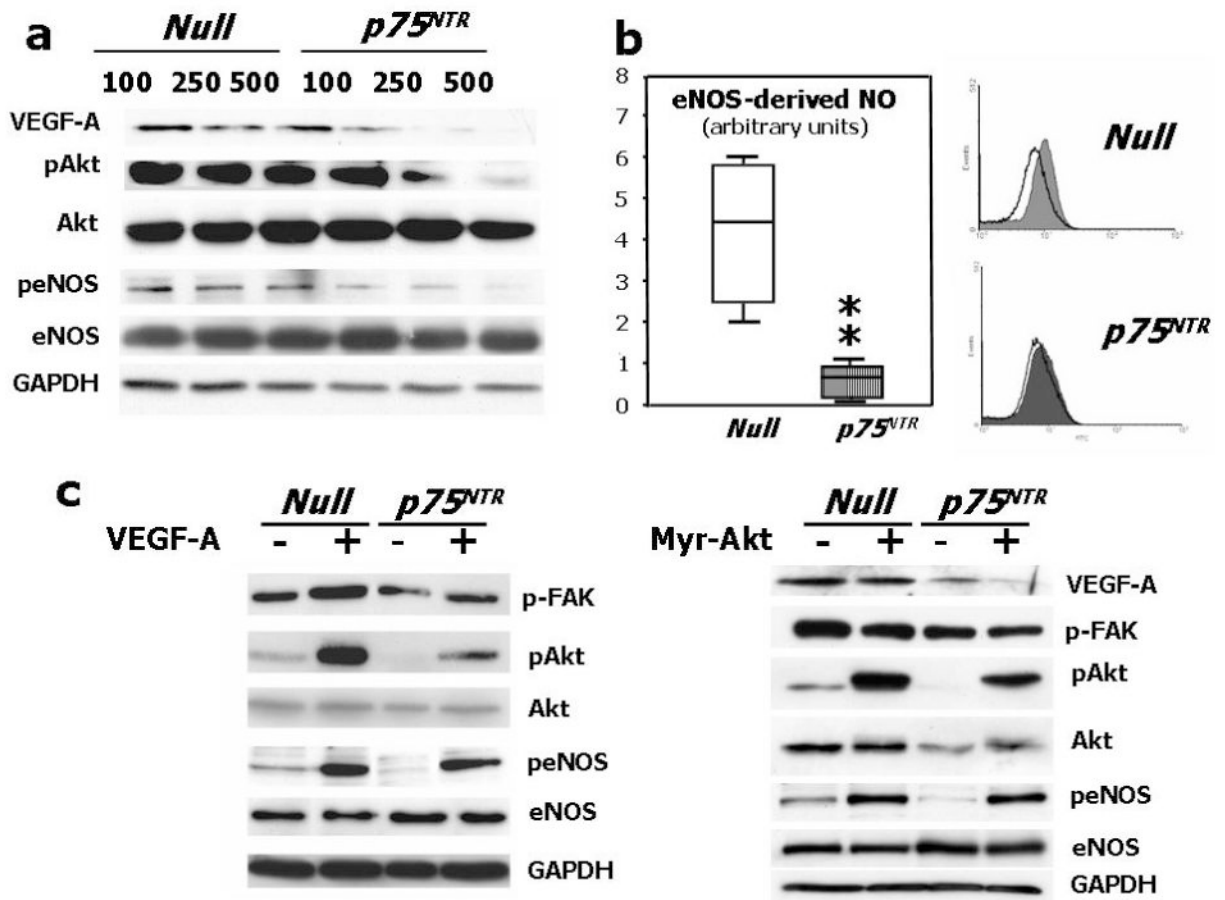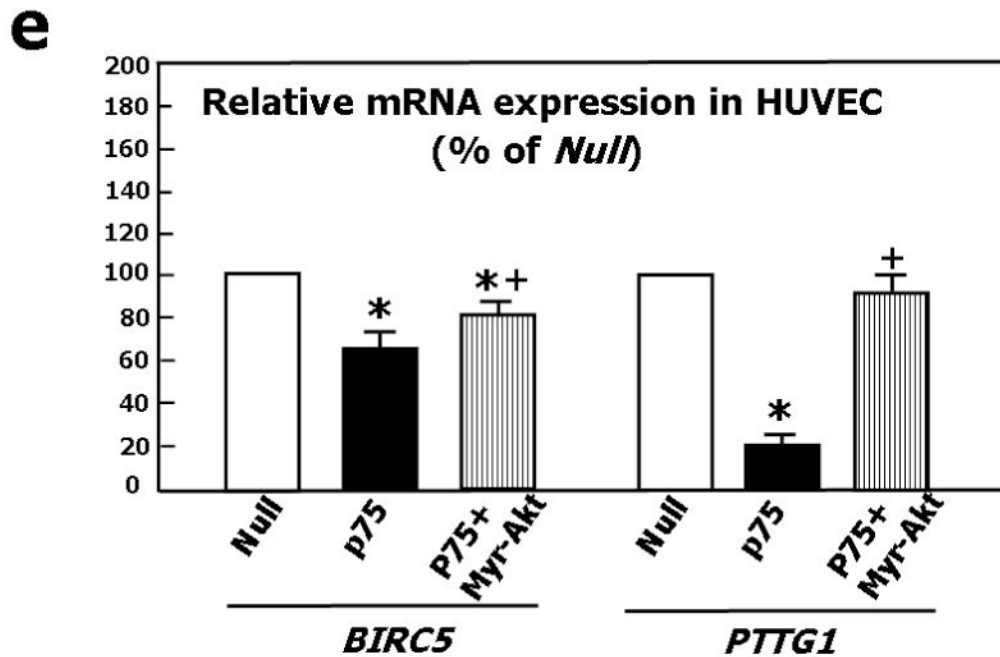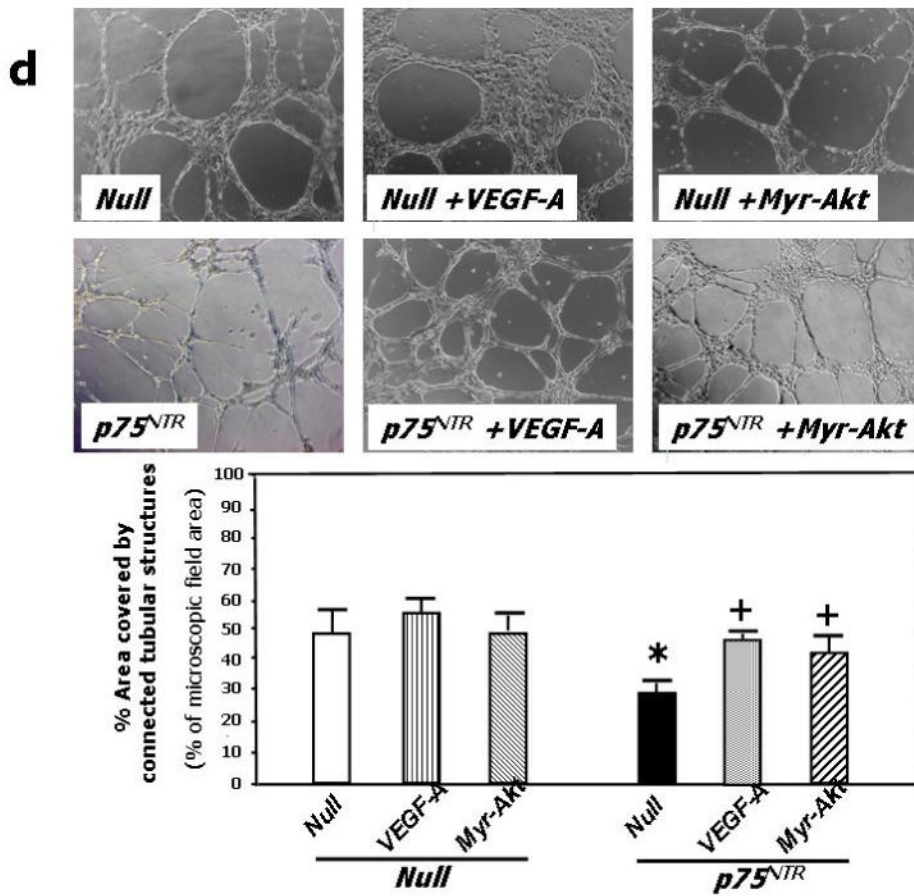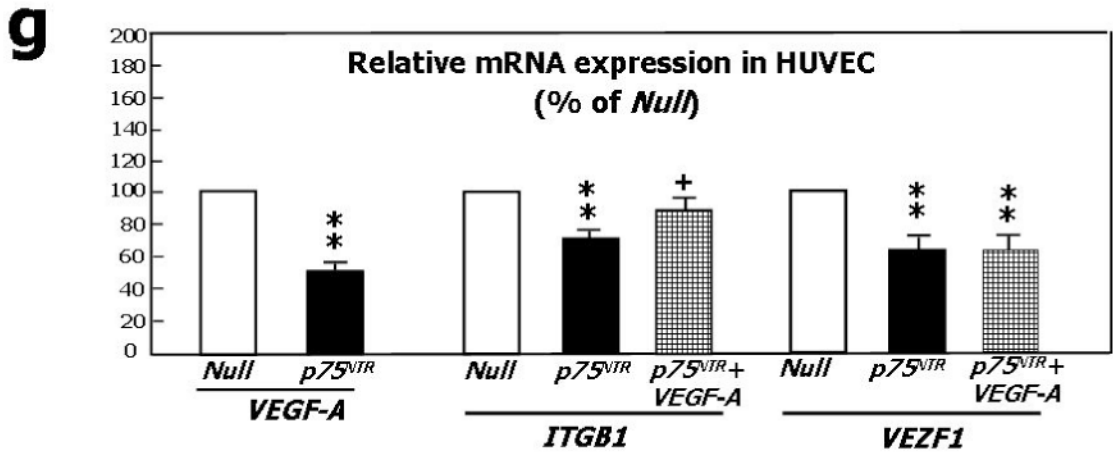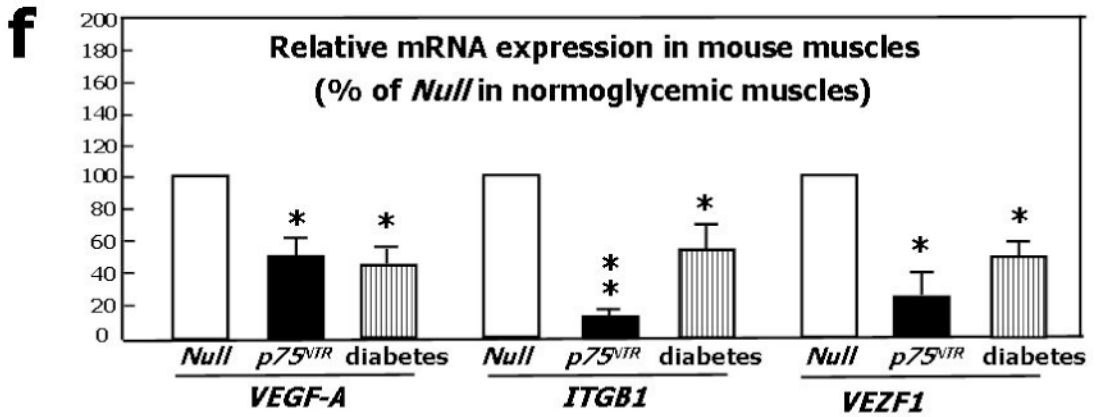
Fig. 3. p75^NTR inhibits pro-angiogenesis and pro-survival pathways in EC and mouse limb muscles

(a) Western blotting showing protein expression of VEGF-A, phospho-Akt, total Akt, phospho-eNOS, and total eNOS. GAPDH was used as loading control. HUVEC were infected with *Ad.Null* or *Ad.p75^NTR* (100, 250, and 500 M.O.I.) and then lysated for western blotting. Bands are representative of three independent experiments. **(b)** HUVEC were infected with *Ad.Null* or *Ad.p75^NTR* (250 M.O.I.). The release of NO was analyzed using the fluorescent probe DAF-2DA in the presence or absence of the eNOS preferential inhibitor L-NIO. FL1 fluorescence, emitted by DAF-2DA after reaction with NO, was determined by FACS. The bar graph shows the NOS-mediated FL1 mean fluorescence intensity after subtraction of eNOS-independent fluorescence emitted in presence of L-NIO. Representative histographs are shown on the right. Full curves are representative of NO release in the absence of L-NIO. Empty curves show NO release in the presence of L-NIO. Values in bar graph are means±SEM **$P<0.01$ vs. *Ad.Null*; **(c)** Left Panel: Protein expression of phospho-FAK, phospho-Akt, total Akt, phospo-eNOS, and total eNOS, in HUVEC infected with *Ad.Null* or *Ad.p75^NTR* (each at 250 M.O.I.) plus *Ad.VEGF-A* or its control *Ad.Null* (each at 10 M.O.I.). GAPDH is used as a loading control. Bands are representative of three independent experiments. Right Panel: Protein expression of VEGF-A, phospho-FAK, total Akt, phospho-Akt, total eNOS, and phospo-eNOS in HUVEC infected with *Ad.Null* or *Ad.p75^NTR* (each at 250 M.O.I.) plus *Ad.Myr-Akt* or its control *Ad.Null* (each at 100 M.O.I.). GAPDH is used as a loading control. Bands are representative of three independent experiments. **(d)** Both *Ad.VEGF-A* and *Ad.Myr-Akt* rescued tube formation capacity of *p75^NTR*-transduced HUVEC. Cells were infected as described in (c) at 12h before being seeded in matrigel. Images were taken at 24h from seeding. Values in the quantification graph are means±SEM.* $P<0.05$ vs. *Ad.Null* plus *Ad.Null,* ^+$P<0.05$ vs. *Ad.p75^NTR* plus *Ad.Null*. **(e)** Relative mRNA expression (determined by real-time RT-PCR, using RNA 18S as reference) of *BIRC5* (*survivin*) and *PTTG1* (*securin*) in *p75^NTR*-HUVEC and *Null*-HUVEC. Co-infection with *Myr-Akt* enhanced *BIRC5* and *PTTG1* content of *p75^NTR*-HUVEC. Values are means±SEM.* $P<0.05$ vs. *Ad.Null,* ^+$P<0.05$ vs. *Ad.p75^NTR*. **(f)** Relative mRNA expression of *VEGF-A*, *ITGB1*, and *VEZF1* in the adductor muscles of normoglycemic mice following its transduction with *Null* (*Null*) or *p75^NTR* (*p75^NTR*) and in *Null*-transduced diabetic limb muscles (diabetes). Values are means±SEM.*$P<0.05$ and **$P<0.01$ vs. *Ad.Null* in normoglycemic muscles. **(g)** Relative mRNA expression of *VEGF-A*, *ITGB1*, and *VEZF1* in *p75^NTR*-HUVEC and *Null*-HUVEC. Co-infection with *VEGF-A* rescued the mRNA level of *ITGB1* but not of *VEZF1* in *p75^NTR*-HUVEC. Values are means ±SEM.** $P<0.01$ vs. *Ad.Null,* ^+$P<0.05$ vs. *Ad.p75^NTR*. **(h)** Schematic representation of the molecular signalling emanating from p75^NTR in EC.
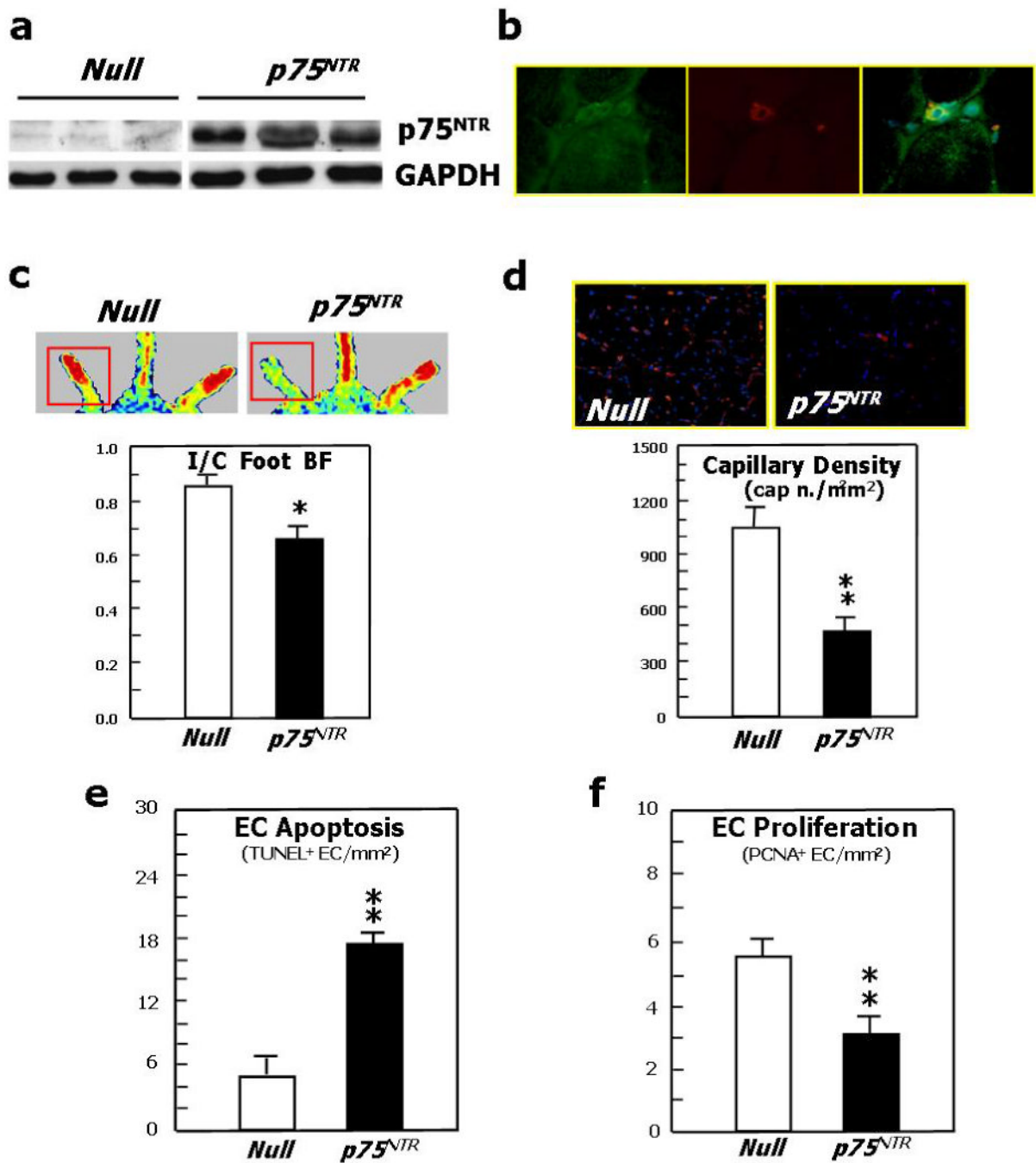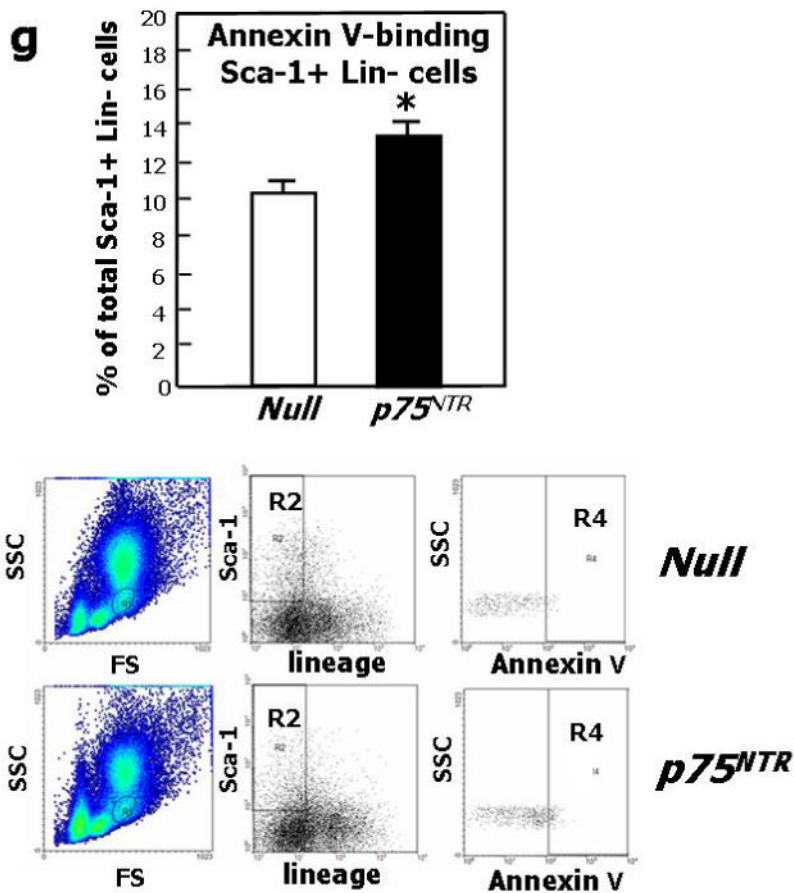
Fig. 4. Forced *p75^NTR* expression inhibits reparative neovascularisation in ischemic limb muscles
(**a**)Western blot analysis showing p75^NTR expression by ischemic murine limb muscles previously infected with *Ad.p75^NTR* (10^9 p.f.u.). (**b**) Staining of muscular section with an antibody for V5 (green fluorescence) and with the endothelial marker isolectin-B4 (red fluorescence) shows that muscular capillary EC express the transgene (yellow fluorescence, from merging) following infection of muscles with *Ad.p75^NTR* (V-5 tagged). (**c**) Recovery of the blood flow (BF) to the ischemic foot (expressed as the ratio between BF in the ischemic to BF in the contra-lateral foot) at 14d after ischemia induction and intramuscular gene transfer with *Ad.p75^NTR* or *Ad.Null*. Values are means±SEM. *P<0.05 vs. *Ad.Null*. Representative laser Doppler images taken at 14d post-ischemia induction are also shown. Squares include the area of interest, where blood perfusion was calculated. Color scale from blue to brown indicates progressive increases in BF; (**d**) Capillary density of ischemic adductor muscles of mice described in (c). Values are means±SEM. **P<0.01 vs. *Ad.Null*. Images in upper panels show muscles stained with isolectin B4 (red fluorescence) to recognize EC and counterstained with DAPI (blue fluorescence) to recognize nuclei; (**e**) Apoptosis (revealed by TUNEL assay) and (**f**) proliferation (revealed by immunhistochemistry for the proliferating cell antigen PCNA) of EC in limb muscles at 5d post-ischemia induction and gene transfer. Values are means±SEM. **P<0.01 vs. *Ad.Null*; (**g**) the percentage of BM-resident Sca-1^+Lin^-progenitor cells undergoing apoptosis (recognized by Annexin-V staining) increased in response to transduction of ischemic muscles with *p75^NTR*. Values are means±SEM. *P<0.05 vs. *Ad.Null*; (**h**) Representative examples of FACS analyses are shown for BM-MNC taken from ischemic limbs previously infected with *Ad.p75^NTR* or *Ad.Null*. First, monocytic cells were

identified by size/granularity (left panel), followed by selection of Sca-1^{+}Lin^{-}cells (R2, central panel). Finally, the percentage of Annexin-V-positive cells was calculated (R4, right panel).
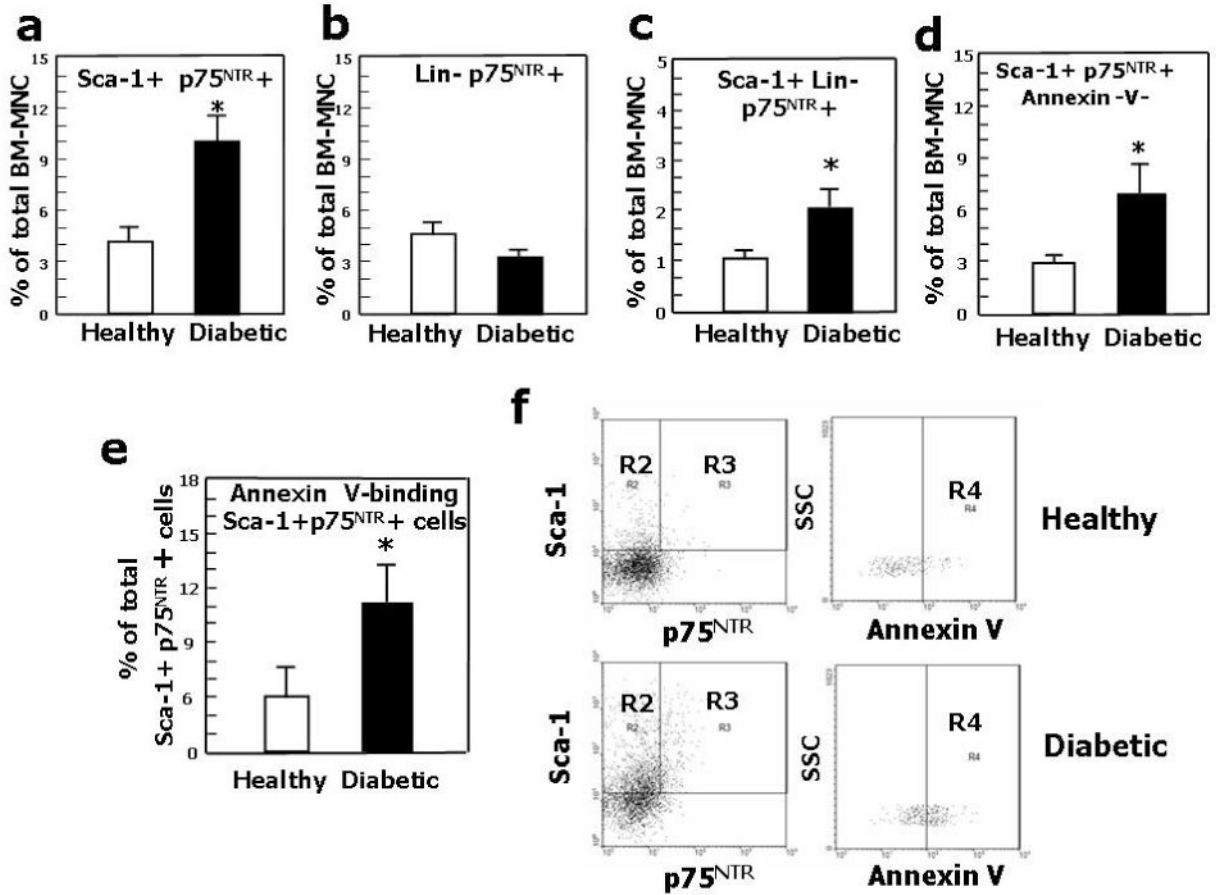
Fig. 5. Diabetes increases p75^{NTR} in BM progenitor cells
(**a**), (**b**), The percentage of BM-MNC co-expressing Sca-1 and p75^{NTR} (a)increased in diabetic mice, while the percentage of BM-MNC Lin$^-$ cell expressing p75^{NTR} (b) did not change. (**c**) The percentage of Sca-1$^+$ Lin$^-$ p75^{NTR+} increased in diabetic BM-MNC. (**d**) The percentage of Sca-1$^+$p75^{NTR+}Annexin-V$^+$ cells increased in diabetic BM-MNC. (**e**) The percentage of Sca-1$^+$p75^{NTR+} cells undergoing apoptosis (recognized by Annexin-V staining) increased in the BM-MNC of diabetic mice. Values are means±SEM. *P<0.05 vs. healthy mice. (**f**) Identification of apoptotic cells (gate R4) among Sca-1$^+$p75^{NTR+} (gate R3) BM-MNC. After selection of monocytic cells according to size and granularity (not shown) and further identification of Sca-1$^+$p75^{NTR+} cells (left panel), positivity for Annexin-V was assessed (right panel) in cells derived from healthy or diabetic mice.
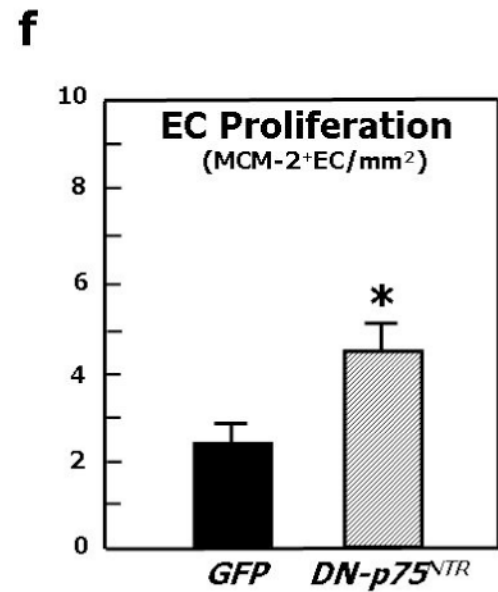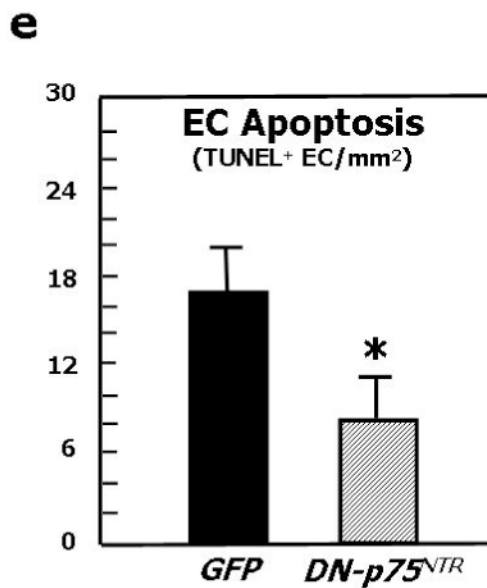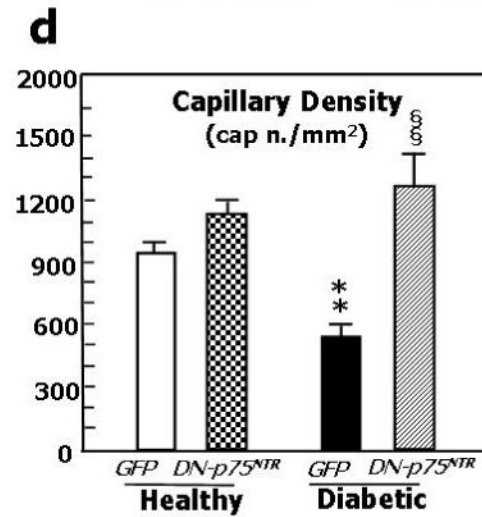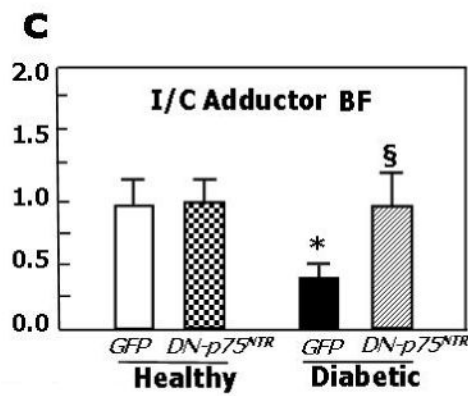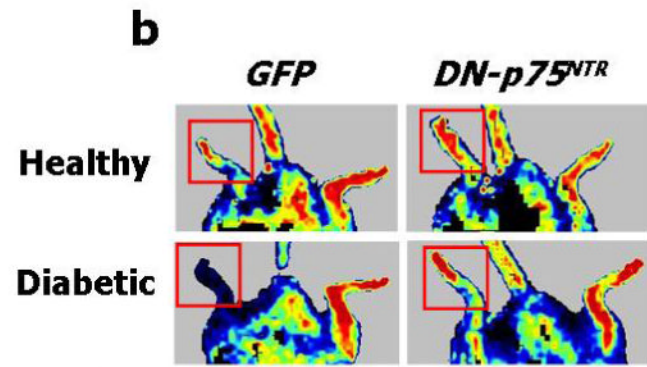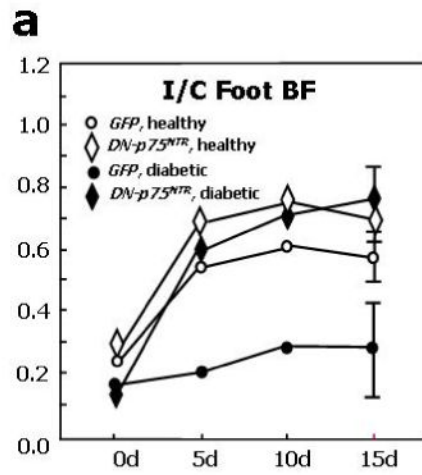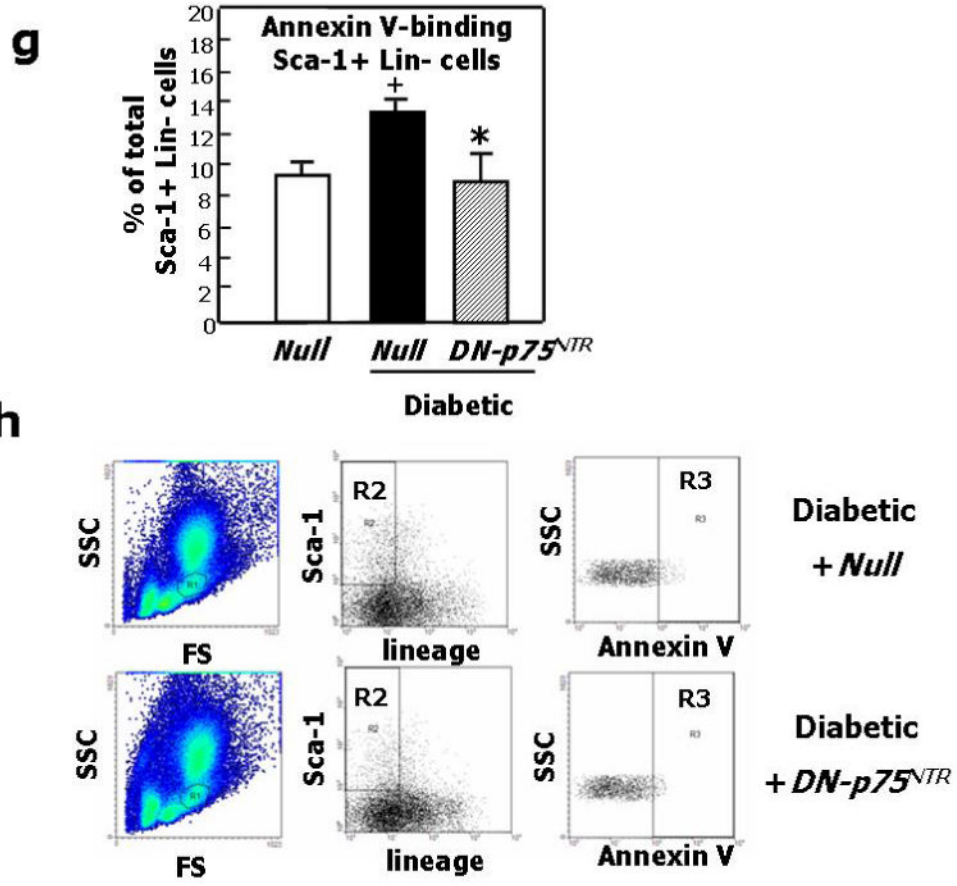
Fig. 6. Inhibition of p75^NTR signalling in diabetic limb muscles restores proper neovascularisation and BF recovery following limb ischemia

Unilateral limb ischemia was induced in diabetic and normoglycemic mice before an adenovirus carrying a dominant negative mutant of p75^{NTR} (*Ad.DN-p75^{NTR}*) or *Ad.GFP* was delivered to the ischemic adductor. (**a**) Time-course of post-ischemic BF recovery (calculated by laser colour doppler) in diabetics and normoglycemic mice treated with *Ad.DN-p75^{NTR}* or *Ad.GFP*; (**b**) Representative laser Doppler images taken at 14d after induction of ischemia are shown. Squares include the area of interest**; (c)** Recovery of BF (measured by Oxford Optronic) to the ischemic adductor (expressed as the ration between BF in the ischemic to BF in the contra-lateral muscle) at 14d after ischemia induction. Values are mean±SEM. *P<0.05 vs. healthy with *Ad.GFP*, §P<0.05 versus diabetic with *Ad.GFP*. (**d**) Capillary density in the ischemic adductor at 14d post-ischemia. Values are means±SEM. **P<0.01 vs. healthy with *Ad.GFP*, §§P<0.05 vs. diabetic with *Ad.GFP*. (**e**) Apoptosis (revealed by TUNEL assay) and (**f**) proliferation (revealed by immunhistochemistry for the proliferation antigen MCM-2) of capillary EC in diabetic limb muscles at 14d post-ischemia induction. Values are means±SEM. *P<0.05 vs. *Ad.GFP*. (**g**) The percentage of BM-resident Sca-1^{+}Lin^{-} progenitor cells undergoing apoptosis (recognized by Annexin-V staining) is significantly reduced by intramuscular delivery of *Ad.DN-p75^{NTR}* in diabetic mice. Values are means±SEM. $^{+}$P<0.05 vs. healthy with *Ad.Null*.*P<0.05 vs. diabetic with *Ad.Null*. (**h**) Representative examples of FACS analyses of diabetic BM are shown. First, monocytic cells were identified by size/ granularity (left panel), followed by selection of Sca-1^{+}Lin^{-} cells (R2, central panel). Finally, the percentage of cells positive for Annexin-V was calculated (R4, right panel).